N89-20955

TEST TECHNIQUES
A Survey Paper on Cryogenic Tunnels, Adaptive Wall Test Sections, and Magnetic Suspension and Balance Systems

Robert A. Kilgore, David A. Dress and Stephen W.D. Wolf*
Experimental Techniques Branch
NASA Langley Research Center
Hampton, Virginia

Colin P. Britcher
Department of Mechanical Engineering and Mechanics
Old Dominion University
Norfolk, Virginia

SUMMARY

Our ability to get good experimental data in wind tunnels is often compromised by things seemingly beyond our control. Inadequate Reynolds number, wall interference, and support interference are three of the major problems in wind tunnel testing.

Techniques for solving these problems are available. Cryogenic wind tunnels solve the problem of low Reynolds number. Adaptive wall test sections can go a long way toward eliminating wall interference. A magnetic suspension and balance system (MSBS) completely eliminates support interference. We are beginning to realize the potential of these techniques.

This survey paper covers cryogenic tunnels, adaptive wall test sections, and MSBS. We give a brief historical overview and describe the present state of development and application in each area. Finally, we attempt to predict future developments and applications of these test techniques.

INTRODUCTION

There are many reasons why we want good data from our wind tunnels. However, problems with wind tunnels often keep us from getting the quality of data we need. Any list of problems with wind tunnels would include **inadequate Reynolds number, wall interference**, and **support interference**. Fortunately, techniques for solving these major problems are available.

Earlier in this Symposium, Wayne McKinney gave the status of the U.S. National Transonic Facility (NTF) and described the early test results. The NTF is an excellent example of the use of a cryogenic wind tunnel to solve the problem of low Reynolds number. In this survey paper we give information on several other cryogenic tunnels.

We also describe solutions to two other major problems with wind tunnels, wall and support interference. Adaptive wall test sections, first used in the 1930s, go a long way toward getting rid of wall interference. Magnetic suspension of the model, first used in the 1950s, completely eliminates support interference.

The three sections of this paper cover cryogenic tunnels, adaptive wall test sections, and magnetic suspension and balance systems. Each section gives a brief historical overview and describes the present state of development and application. Finally, we predict a bright future for the continued rapid development and application of these test techniques.

* NRC Associate

CRYOGENIC WIND TUNNELS

The world's first cryogenic wind tunnel was built at NASA Langley in 1972. Following the development of this small low-speed tunnel, cryogenic tunnels were built at other research centers. This section describes some of these tunnels.

References 1 and 2 are the two parts of a review article on cryogenic tunnels published in *Cryogenics* in 1984. Reference 1 gives the evolution, theory, and advantages of cryogenic tunnels. Reference 2 describes the early use of cryogenic tunnels in the United States at NASA Langley. Reference 2 also briefly describes some of the cryogenic tunnel activities around the world.

Work on the development and use of cryogenic tunnels has continued since 1984. Reference 3 is a recent article in *Cryogenics* which gives an update on cryogenic tunnel activities. The emphasis in reference 3 is on the cryogenic engineering aspects of the cryogenic tunnels. We base this present survey paper on reference 3. However, the emphasis in this survey paper is on the aerodynamic capabilities of the cryogenic tunnels.

We do not attempt to describe every cryogenic tunnel. Rather, we describe selected tunnels to give a general idea of activities around the world. These tunnels also illustrate the wide variety of cryogenic tunnels built since 1972.

England
Royal Aircraft Establishment - Bedford
Cryogenic Test Duct

Law and his colleagues at the Royal Aircraft Establishment (RAE) in Bedford built a simple closed circuit wind tunnel called the Cryogenic Test Duct. The Cryogenic Test Duct is part of the United Kingdom support for the European Transonic Windtunnel (ETW) program.[4]

The photograph in figure 1 shows the general arrangement of the RAE Cryogenic Test Duct. This photograph shows the uninsulated Test Duct. Table 1 gives the basic features of the Cryogenic Test Duct.

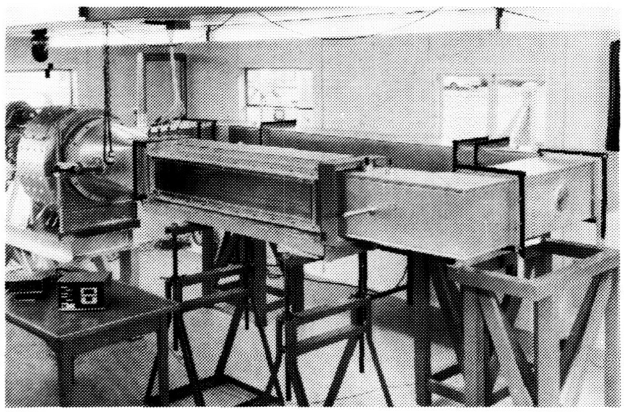

Fig. 1 - Photograph of RAE - Bedford Cryogenic Test Duct.

The 1:1 contraction is a clear sign the Test Duct is not designed for aerodynamic research. However, the Test Duct is ideally suited to provide the required cryogenic gas flow needed to test balances and model components. The Test Duct is simple in both design and construction. A heating and air conditioning shop in Bedford built the Test Duct for RAE.

The Test Duct has a simple calibration device for loading wind tunnel balances mounted in the test section. The test section has transparent side walls which allow direct visual observation during tests. The use of internal insulation permits rapid changes in the operating temperature. Reference 4 gives more details on the design and operation of the RAE Cryogenic Test Duct.

TABLE 1.- Cryogenic Test Duct at RAE-Bedford (England)

Type	closed circuit, centrifugal fan
Material of construction	aluminum
Insulation	external and internal
Cooling	liquid nitrogen
Test gas	nitrogen
Test section size (h,w,l)	0.3 x 0.3 x 1.5 m
Speed range	up to 25 m/s
Contraction ratio	1:1
Stagnation pressure	atmospheric
Stagnation temperature	90 K - ambient
Running time	typically 1 hour
Max. Reynolds number/m	11.4 million
Drive motor	9 kW
Fan speed	up to 2500 rpm
LN_2 tank volume	1.28 m^3

ORIGINAL PAGE IS
OF POOR QUALITY

University of Southampton
0.1 m Cryogenic Wind Tunnel

Figure 2 shows a photograph of the 0.1 m Cryogenic Wind Tunnel at Southampton.[5] Table 2 gives the basic features for this low-speed tunnel.

Goodyer and his colleagues have used the low-speed tunnel at Southampton for a variety of purposes. These range from searching unsuccessfully for temperature spottiness (thermal turbulence) to successfully developing flow visualization techniques. In 1977, Kell used this tunnel to develop a surface flow visualization technique using liquid propane carrying a pigment.[6] He and Goodyer also found they could use a variety of tuft materials, including wool and cotton, even at 79 K.

Since first running in 1977, several improvements have made this simple cryogenic tunnel a very useful research tunnel.[7] For example, the tunnel now has automatic controls able to hold either Mach number or Reynolds number constant.[8]

Goodyer added three 1 kW electric heaters to the circuit to speed up the warming of the tunnel following cryogenic operation. The heaters also provide close temperature control. The technique is to inject a slight excess of liquid nitrogen over the amount required to balance heat added by the fan. Modulation of the heaters controls temperature to ±0.5 K.

By adding to the heat from the fan, the heaters also make it possible to run at temperatures up to 380 K. The ability to run at high temperatures gives an increased range of test Reynolds numbers. The test gas is usually air when operating at room temperatures or above.

After modifying the tunnel in 1978, Britcher used it with the Southampton 6-component Magnetic Suspension and Balance System (MSBS).[9] We will tell you more about the Southampton MSBS later in this paper.

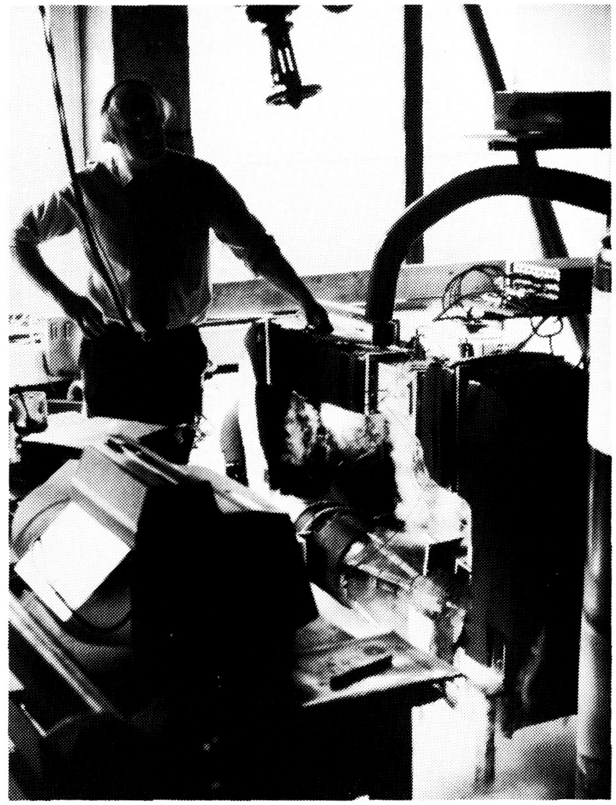

Fig. 2 - 0.1m Cryogenic wind tunnel at Southampton.

TABLE 2.- Cryogenic Low-Speed Tunnel at Southampton (England)

Type	closed circuit, fan
Material of construction	mostly aluminum
Insulation	external
Cooling	liquid nitrogen
Test gas	nitrogen; air (when running hot)
Test section size (h,w,l)	
Regular	0.11 x 0.11 x 0.25 m
MSBS	0.14 x 0.11 x 0.41 m
Speed range	14 - 72 m/s
Mach range	0.04 - 0.40
Contraction ratio	5.4:1
Stagnation pressure	atmospheric
Stagnation temperature	79 - 380 K
Running time	typically 1 hour
Max. Reynolds number/m	50 million
Drive motor	4 kW
Fan speed	up to 7200 rpm
LN_2 tank volume	0.17 m^3

Europe
European Transonic Windtunnel - Köln

Four European countries have joined through AGARD to design and build a large fan-driven transonic cryogenic tunnel. The tunnel is the European Transonic Windtunnel (ETW). The countries funding the ETW are France, the Federal Republic of Germany, the Netherlands, and the United Kingdom. These countries expect the ETW to meet their transonic high Reynolds number testing needs. Table 3 gives the major design features of the ETW.

Each of the four countries is doing research in support of the design and use of the ETW. Sverdrup Corporation has completed the preliminary design of the ETW.

The DFVLR center at Porz-Wahn (near Köln) is the site selected for the ETW. Construction of the ETW will start later this year. Reference 10 gives a complete account of the evolution and status of the ETW project.

Pilot European Transonic Windtunnel (PETW), NAL - Amsterdam

Work on the ETW includes building a 1:8.8 scale pilot tunnel at the National Aerospace Laboratory (NAL) in Amsterdam.[10] The pilot tunnel, known as PETW, has the same operating ranges as proposed for the ETW.

One big difference between the PETW and the ETW is the type of thermal insulation. The PETW is inside an insulated room. The latest design for the ETW calls for internal thermal insulation similar to the insulation used in the U.S. NTF. Table 4 gives the major design features of the PETW.

Researchers at NAL are using the PETW to check the aerodynamic performance of the ETW design. In addition, they are using the PETW to make control studies and gain operational experience.

France
ONERA-CERT - Toulouse
T2 Cryogenic Induction Tunnel

Mignosi and his colleagues at ONERA-CERT modified an injector driven tunnel, T2, for cryogenic operation. They also fitted the T2 with an adaptive wall test section.

The cryogenic modification followed development work in a 1:4 scale model pilot tunnel, T'2. Reference 11 gives a complete description of this work. Figure 3 shows a photograph of the T2. Table 5 gives the main features of the T2.

The T2 and the T'2 are the only cryogenic tunnels driven by induction. The induction drive of the T2 is in the seven turning vanes of the first corner. The hollow vanes receive high pressure dry air which blows through the trailing edges.

TABLE 3.- European Transonic Windtunnel (ETW) at DFVLR Porz-Wahn (W. Germany)

Type	closed circuit, fan
Material of construction	stainless steel
Insulation	internal
Cooling	liquid nitrogen
Test gas	nitrogen
Test section size (h,w,l)	2.0 x 2.4 x 6.9 m
Mach range	0.15 - 1.3
Contraction ratio	12:1
Stagnation pressure	1.25 - 4.5 bars
Stagnation temperature	90 - 313 K
Running time	typically 10 min
Max. Reynolds number/m	228 million
Drive motor	50 MW
Fan speed	up to 1200 rpm
LN_2 tank volume	3000 m^3

TABLE 4.- Pilot European Transonic Windtunnel (PETW) at NAL-Amsterdam (The Netherlands) (1:8.8 version of ETW)

Type	closed circuit, fan
Material of construction	aluminum alloy
Insulation	external, cold box
Cooling	liquid nitrogen
Test gas	nitrogen
Test section size (h,w,l)	0.23 x 0.27 x 0.78 m
Mach range	0.35 - 1.0 continuous 1.20, 1.35 fixed nozzles
Contraction ratio	12:1
Stagnation pressure	1.25 - 4.5 bars
Stagnation temperature	90 - 313 K
Running time	typically 60 min
Max. Reynolds number/m	228 million
Drive motor	1 MW
Fan speed	up to 9000 rpm
LN_2 tank volume	28.5 m^3

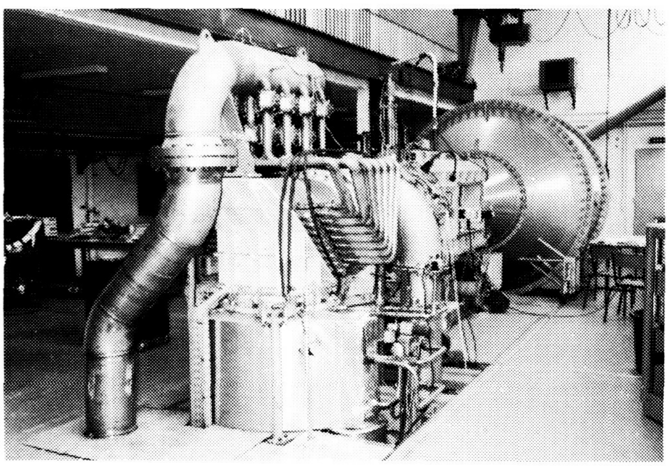

Fig. 3 - T2 cryogenic tunnel, ONERA/CERT.

A digital computer controls the tests in the T2. During a typical airfoil test, they program the computer to cool the stream to 20 K below the intended operating temperature. This under-cooling quickly drives the model to the adiabatic temperature for the intended test conditions. Once the model is at the desired temperature, total pressure and Mach number automatically go to the desired test conditions.

When the test conditions (pressure, temperature, and Mach number) are stable - a matter of only a few seconds - the solid upper and lower test section walls iterate to an interference free condition. Finally, the computer records the model and tunnel wall data. It takes only about 5 minutes from the beginning of a run until they have plotted airfoil data.

TABLE 5.- T2 Cryogenic Tunnel at ONERA/CERT (France)

Type	closed circuit, induction
Material of construction	mild & stainless steels
Insulation	internal
Cooling	liquid nitrogen
Test gas	nitrogen rich air
Test section size (h,w,l)	0.37 x 0.37 x 1.32 m (solid adaptive walls)
Mach range	0.3 - 1
Contraction ratio	20:1
Stagnation pressure	1.6 - 3.5 bars
Stagnation temperature	95 K - ambient
Running time	up to 100 sec +
Max. Reynolds number/m	340 million
LN_2 tank volume	20 m^3

<u>T'3 Cryogenic Fan-Driven Tunnel</u>

There have been additional cryogenic tunnel projects in support of ETW at ONERA-CERT. One of these projects is the T'3 Cryogenic Tunnel, first operated in 1980.[12] The fan-driven T'3 gave valuable information on the design and operation of fan-driven cryogenic tunnels.

The T'3 also has an adaptive-wall test section. The walls of the 10 by 12 cm test section are manually adjusted to the desired streamline shapes. Table 6 gives the main features of the T'3.

TABLE 6.- T'3 Cryogenic Tunnel at ONERA/CERT (France)

Type	closed circuit, fan
Material of construction	stainless steels
Insulation	internal
Cooling	liquid nitrogen
Test gas	nitrogen
Test section size (h,w,l)	0.10 x 0.12 x 0.60 m (solid adaptive walls)
Mach range	0.05 - 0.80
Contraction ratio	13.3:1
Stagnation pressure	1.0 - 4 bars
Stagnation temperature	95 K - ambient
Running time	up to 25 minutes
Max. Reynolds number/m	340 million
Drive motor	125 kW
Fan speed	up to 9800 rpm
LN_2 tank volume	0.58 m^3

Germany
DFVLR
<u>Kryo-Kanal-Köln (KKK) at Köln</u>

Viehweger and his co-workers at the DFVLR Research Center at Porz-Wahn modified a 3 m low-speed tunnel for cryogenic operation.[13] The project started in 1978 with studies of how to modify the tunnel.

The studies included modeling the liquid nitrogen injection process and finding ways of fixing internal insulation to the concrete tunnel. They completed modifications to the tunnel in March of 1985. The first cryogenic operation was in January of 1986.

The Kryo-Kanal-Köln (KKK) is a modern, closed circuit, fan-driven cryogenic tunnel with automatic control of the test conditions. Figure 4 shows an aerial view of the KKK. Table 7 gives the main features of the KKK.

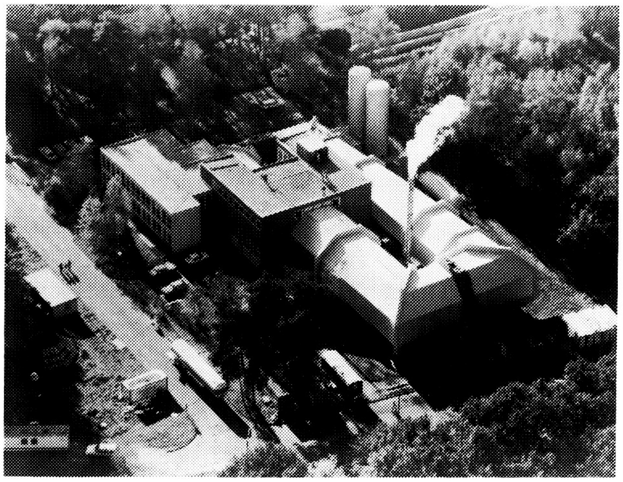

Fig. 4 - Kryo-Kanal-Köln at DFVLR-Köln.

ORIGINAL PAGE
BLACK AND WHITE PHOTOGRAPH

For model changes or modification, there is an access lock and model conditioning room below the test section. Following a run, the model and its support are moved from the test section into the lock.

For major model changes, warm gaseous nitrogen is blown into the closed lock and warms everything to ambient temperature. Fans blow dry air into the lock before the technicians enter to work on the model. The access time is about 4 hours because of the long warm up time for the model support and lifting systems.

For minor changes to the model, the model is moved into the conditioning room. In this relatively small room, warm-up of the model takes only about 30 minutes. A microcomputer controls all model movements in the lock or the conditioning room.

TABLE 7.- Kryo Kanal Köln (KKK) at DFVLR - Köln (W. Germany)

Type	closed circuit, fan
Material of construction	concrete
Insulation	internal
Cooling	liquid nitrogen
Test gas	nitrogen
Test section size (h,w,l)	2.4 x 2.4 x 5.4 m
Mach range	up to 0.38
Contraction ratio	10.3:1
Stagnation pressure	up to 1.12 bars
Stagnation temperature	100 - 300 K
Running time	up to several hours
Max. Reynolds number/m	37 million
Drive motor	1 MW
Fan speed	up to 1000 rpm
LN_2 tank volume	150 m^3

<u>Cryogenic Ludwieg Tube Tunnel at Göttingen</u>

Hefer and his colleagues at DFVLR Göttingen recently brought on line a cryogenic Ludwieg tube tunnel (CLTT). The sketch in Figure 5 shows the layout of the CLTT. Table 8 gives the major design features of the CLTT. Reference 14 describes the design and operation of the CLTT.

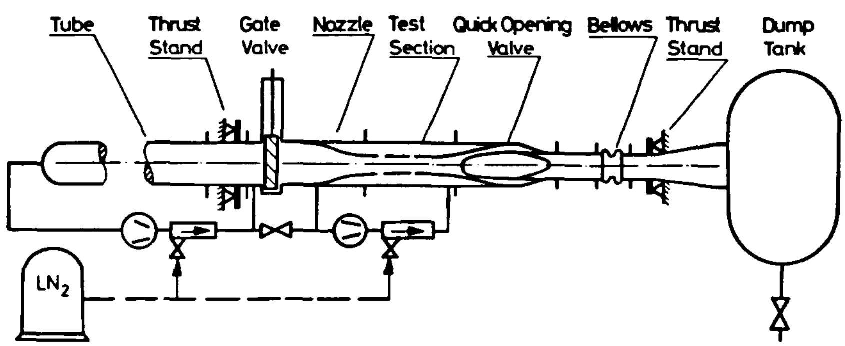

Fig. 5 - Cryogenic Ludwieg Tube Tunnel at DFVLR-Göttingen.

One big advantage seen for the Ludwieg tube tunnel is good flow quality. We expect the researchers at DFVLR Göttingen to use the high Reynolds number capability and good flow quality to develop advanced airfoils.

The present test section of the CLTT has conventional slotted walls. However, Hefer and his colleagues plan to install an adaptive-wall test section as soon as possible.

The proposed adaptive-wall test section will have solid but flexible top and bottom walls. In a slight departure from conventional design, the proposed adaptive-wall test section will have slotted side walls. This arrangement will let them test 3-D models with either adaptive or slotted walls by rotating the plain of symmetry of the models.

TABLE 8.- Cryogenic Ludwieg Tube Tunnel at DFVLR - Göttingen (W. Germany)

Type	Ludwieg tube
Material of construction	stainless steel
Insulation	external
Cooling	liquid nitrogen
Test gas	nitrogen
Test section size (h,w,l)	0.35 x 0.40 x 2.0 m
Mach range	0.25 - 1.0
Charge tube pressure	12.5 bars
Stagnation pressure	up to 10 bars
Stagnation temperature	120 K to ambient
Running time	0.6 to 1.0 sec
Max. Reynolds number/m	400 million
LN_2 tank volume	25 m^3

Japan

There is a lot of cryogenic tunnel activity in Japan. In October of 1987, one of the authors (Kilgore) visited Japan and saw their cryogenic tunnels. He met the people who designed, built, and use the cryogenic tunnels. He also observed two of the tunnels operating.

National Aerospace Laboratory (NAL)
0.1 x 0.1 m Pilot Transonic Cryogenic Tunnel

One company, Ishikawajima-Harima Heavy Industries Company, Limited (IHI) has been the general contractor for the cryogenic tunnels built in Japan. In 1982 IHI designed and built the 0.1 x 0.1 m Pilot Transonic Cryogenic Tunnel for NAL. Figure 6 is a photograph of the NAL cryogenic tunnel. Table 9 gives the main features of the NAL cryogenic tunnel.

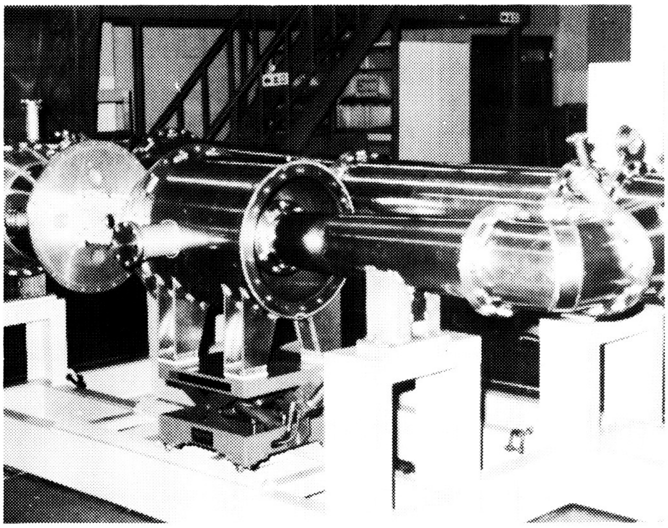

Fig. 6 - Pilot Transonic Cryogenic Tunnel at NAL.

Sawada and his colleagues at NAL use this small tunnel for aerodynamic studies and to gain operational experience. They also use it to support design studies of a larger transonic cryogenic tunnel for Japan. References 15 and 16 give details on the construction and performance of this closed circuit, fan driven tunnel.

Two 6 cm diameter glass windows allow a clear view into the test section. These windows use a vacuum space for thermal insulation rather than the more conventional dry nitrogen purging system.

TABLE 9.- Pilot Transonic Cryogenic Tunnel at NAL (Japan)

Type	closed circuit, fan
Material of construction	A5052 Al-alloy
Insulation	external, purged
Cooling	liquid nitrogen
Test gas	nitrogen
Test section size (h,w,l)	0.1 x 0.1 x 0.3 m
Mach range	up to 1.02
Contraction ratio	18:1
Stagnation pressure	up to 2 bars
Stagnation temperature	90 K - ambient
Running time	more than 2 hours
Max. Reynolds number/m	130 million
Drive motor	55 kW
Fan speed	600 - 5700 rpm
LN_2 tank volume	2.17 m^3

The 0.1 x 0.1 m tunnel at NAL has a modern digital control and data acquisition system. The researchers at NAL make excellent use of a color video display during all phases of the operation. The computer displays check sheets and prompts to the operator during start up. The computer also displays the tunnel conditions during the run. The interactive design of the control and data acquisition computer makes tunnel operation simple and straightforward.

Sawada and his colleagues have made many aerodynamic tests and explored the entire operating envelope of the tunnel. They determined tunnel features such as power factor and transient responses to changes in fan speed and liquid nitrogen flow rate. In all respects, the NAL cryogenic tunnel works satisfactorily and as predicted.

The NAL cryogenic tunnel usually runs 2 days each week. Since first operated in 1984, it has accumulated slightly over 400 hours of running.

Plans for the 0.1 x 0.1 m tunnel include aerodynamic tests on some simple models using a heated three-component strain gage balance.

University of Tsukuba

The Institute of Engineering Mechanics at the University of Tsukuba has two low-speed cryogenic tunnels. One has a 0.1 x 0.1 m test section and the other a 0.5 x 0.5 m test section.

0.1 x 0.1 m Low-Speed Cryogenic Tunnel

The 0.1 x 0.1 m low-speed cryogenic tunnel first ran at cryogenic temperatures in 1980. Adachi and his colleagues have used this tunnel to calibrate sensors and to gain experience with cryogenic tunnels. This tunnel also gave design information for the larger low-speed tunnel at Tsukuba.

Because of the small size of the 0.1 x 0.1 m tunnel, it is no longer used for aerodynamic research. Table 10 gives the design features of this tunnel.

0.5 x 0.5 m Cryogenic Tunnel

Figure 7 is a photograph the 0.5 x 0.5 m low-speed tunnel. Table 11 gives the main features of this tunnel.

This tunnel is also a closed circuit, fan-driven tunnel. The maximum operating pressure of this tunnel is quite high at 8.1 bars. A mostly mild steel pressure shell makes this tunnel unique among pressurized continuous-flow cryogenic tunnels. The designers deviated from convention in using mild steel for a cryogenic pressure vessel. They felt safe using mild steel because of the internal insulation system.

Adachi and his colleagues use this tunnel to make a variety of aerodynamic measurements. These include testing various cylinders over a wide range of Reynolds numbers.[17]

National Defense Academy (NDA)
NDA High Reynolds Number Flow Facility

IHI built a cryogenic tunnel for the Department of Aeronautical Engineering of the Japanese National Defense Academy. IHI delivered this tunnel, the NDA High Reynolds Number Flow Facility, in March of 1985. Yamaguchi and his colleagues use this tunnel for basic fluid mechanics studies at the Academy.

TABLE 10.- 0.1 x 0.1 m Cryogenic Low-Speed Tunnel at Tsukuba (Japan)

Type	closed circuit, fan
Material of construction	stainless steel
Insulation	external
Cooling	liquid nitrogen
Test gas	nitrogen
Test section size (h,w,l)	0.1 x 0.1 x 0.3 m
Speed range	up to 30 m/s
Contraction ratio	3.41:1
Stagnation pressure	up to 2 bars
Stagnation temperature	100 K - ambient
Running time	up to 2 hours
Max. Reynolds number/m	30 million
Drive motor	2.2 kW
Fan speed	1500 - 4300 rpm
LN_2 tank volume	0.175 m^3

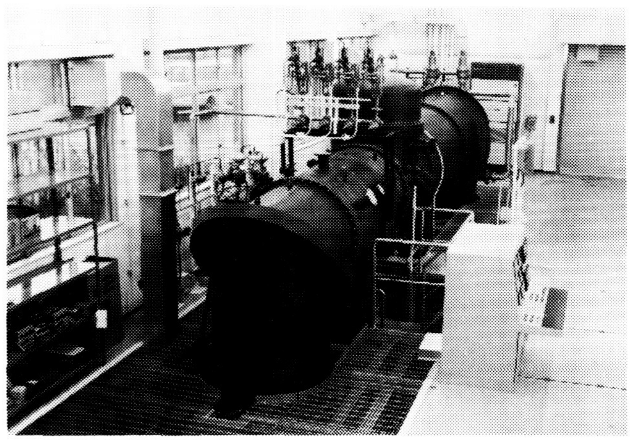

Fig. 7 - 0.5 x 0.5 m Cryogenic Low-Speed Tunnel at Tsukuba.

TABLE 11.- 0.5 x 0.5 m Cryogenic Low-Speed Tunnel at Tsukuba (Japan)

Type	closed circuit, fan
Material of construction	mostly mild steel
Insulation	internal
Cooling	liquid nitrogen
Test gas	nitrogen
Test section size (h,w,l)	0.5 x 0.5 x 1.2 m
Speed range	7 - 65 m/s
Mach range	up to 0.30
Contraction ratio	6.12:1
Stagnation pressure	1.22 - 8.10 bars
Stagnation temperature	118 K - ambient
Running time	30 min. at max. R
Max. Reynolds number/m	200 million
Drive motor	450 kW
Fan speed	150 - 1500 rpm
LN_2 tank volume	20 m^3

Typical of many small tunnels, the plenum of the NDA tunnel mounts on a trolley to allow access to the test section. The test section has two 30 cm diameter optical windows for flow visualization. Table 12 gives the main features of this tunnel.

Yamaguchi and his colleagues completed the initial tunnel calibration in 1985. The exhaust system now includes a precise automatic control valve and a manual control valve. They plan to add automatic control to the liquid nitrogen injection system. They also plan to add an automatic Mach number controller.

TABLE 12.- High Reynolds Number Flow Facility at NDA (Japan)

Type	closed circuit, centrifugal compressor
Material of construction	18-8 stainless steel
Insulation	external
Cooling	liquid nitrogen
Test gas	nitrogen
Test section size (h,w,l)	0.30 x 0.06 x 1.0 m
Speed range	up to 157 m/s
Mach range	up to 0.80
Contraction ratio	14:1
Stagnation pressure	up to 1.77 bars
Stagnation temperature	108 K - ambient
Running time	up to 40 min.
Max. Reynolds number/m	90 million
Drive motor	75 kW
LN_2 tank volume	5 m^3

United States
University of Illinois at Urbana-Champaign (UIUC)
Cryogenic Heat Transfer Tunnel (CHTT)

Clausing and his co-workers at UIUC have built a low-speed fan-driven cryogenic tunnel. They use their cryogenic tunnel for studies of forced, natural, and combined convective heat transfer. The tunnel provides ideal simulation under conditions requiring very large values of both Reynolds number and Grashof number.

The UIUC tunnel fulfills the need of accurately predicting combined convective losses from large, high temperature bodies such as solar "power tower" receivers. For these receivers, the values of both the Grashof and Reynolds numbers are large. Clausing proposed the Cryogenic Heat Transfer Tunnel (CHTT) as an economical way to get the required large values of Grashof and Reynolds numbers.[18] This tunnel also achieves an appropriate and near constant Prandtl number.

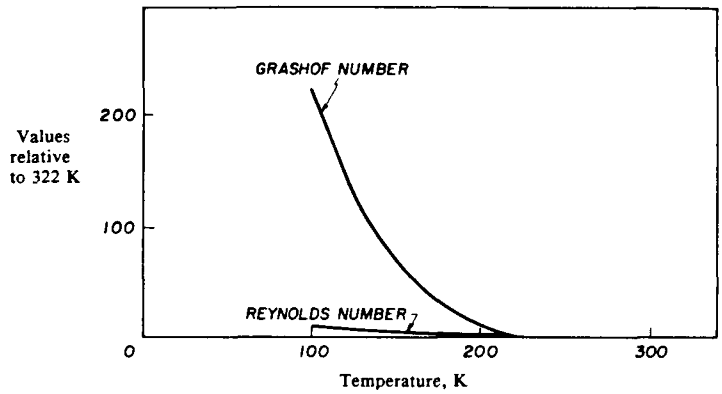

Fig. 8 - Variation of Grashof and Reynolds numbers with temperature.

Figure 8 shows the variations of Grashof number and Reynolds number with temperature. The use of cryogenic temperatures is a good way to get higher Reynolds numbers. It is also an excellent way to get higher Grashof numbers. Furthermore, the cryogenic environment cuts out most of the radiative heat transfer which can cause large errors in natural convection data from conventional facilities. References 19 and 20 discuss both the theory and advantages of the CHTT.

The CHTT is a very successful use of the cryogenic tunnel concept. Table 13 gives the main design features. Reference 21 gives a complete description of this tunnel.

TABLE 13.- Cryogenic Heat Transfer Tunnel at UIUC (USA)

Type	closed circuit, fan
Material of construction	mostly aluminum
Insulation	external, urethane
Cooling	LN_2 heat exchanger with GN_2 injection
Test gas	nitrogen
Test section size (h,w,l)	1.22 x 0.60 x 1.0 m
Speed range	0 - 8 m/s
Contraction ratio	1:1
Stagnation pressure	atmospheric
Stagnation temperature	80 - 300 K
Running time	several minutes
Max. Reynolds number/m	4 million
Drive motor	11.2 kW
Fan speed	0 - 1750 rpm
LN_2 tank volume	1 m^3

NASA Langley
0.3-m Transonic Cryogenic Tunnel

The Low-Speed Cryogenic Tunnel studies ended in the summer of 1972.[22, 23] We then built a small fan-driven transonic cryogenic pressure tunnel. Our desire was to extend our cryogenic tunnel experience to the pressures and speeds needed for a large transonic high Reynolds number cryogenic tunnel.

The design of the Pilot Transonic Cryogenic Tunnel began in December of 1972. It first ran in August of 1973. The first run at cryogenic temperatures was made on October 16, 1973. This was less than 2 years after work started at Langley on cryogenic tunnels.

The Pilot Transonic Cryogenic Tunnel fulfilled its original purpose, that is it proved cryogenic tunnels could work at transonic speeds. In 1976 NASA designated this pilot tunnel a proper NASA facility and renamed it the Langley 0.3-m Transonic Cryogenic Tunnel (0.3-m TCT).

The 0.3-m TCT now sees service in a wide range of experimental programs. These include research in aerodynamics and cryogenic tunnel technology.[24] The basic structure of the tunnel has not changed in its 14 years of operation. However, in 1976 we replaced the original octagonal test section with a slotted wall rectangular test section.

In 1986 we replaced the rectangular test section with a square test section fitted with adaptive walls. We will describe this new test section later in this paper.

We have made changes to the control, instrumentation, and data acquisition subsystems. We have also made changes to the tunnel operating procedures. The tunnel is under completely automatic control. Separate control loops handle liquid nitrogen injection, gaseous nitrogen exhaust, and Mach number. Other digital controllers handle test section side wall boundary-layer removal and streamlining of the flexible top and bottom walls. We are now integrating the separate tunnel control functions under a single supervisory computer.

Table 14 gives the main operating features of the 0.3-m TCT. Reference 24 gives a complete description of the evolution and status of this tunnel.

TABLE 14.- 0.3-m Transonic Cryogenic Tunnel (TCT) at NASA-Langley (USA)

Type	closed circuit, fan
Material of construction	aluminum
Insulation	external, purged
Cooling	liquid nitrogen
Test gas	nitrogen
Test section size (h,w,l)	33 x 33 x 142 cm (solid adaptive walls)
Mach range	0.05 to ≈ 1.3
Contraction ratio	10.7:1
Stagnation pressure	1.1 - 6.2 bars
Stagnation temperature	78 - 340 K
Running time	up to several hours
Max. Reynolds number/m	400 million
Drive motor	2.25 MW
Fan speed	up to 6500 rpm
LN_2 tank volume	212 m^3

U.S. National Transonic Facility (NTF)

The U.S. National Transonic Facility (NTF) is located at NASA Langley. Design of the NTF started in 1975. It came on line late in 1983. The NTF is the largest transonic cryogenic tunnel.[25,26]

McKinney gave the status of the NTF earlier during this Symposium. Therefore, we will not go into any detail about the status of the NTF in this paper. For completeness, we do include the main features of the NTF in Table 15.

TABLE 15.- U.S. National Transonic Facility (NTF) at NASA-Langley (USA)

Type	closed circuit, fan
Material of construction	304 stainless steel, aluminum
Insulation	internal
Cooling	
Cryogenic mode	liquid nitrogen
Air mode	air/water heat exchanger
Test gas	nitrogen or air
Test section size (h,w,l)	2.5 x 2.5 x 7.62 m
Mach range	0.2 - 1.22
Contraction ratio	15:1
Stagnation pressure	1 - 8.9 bars
Stagnation temperature	78 - 340 K
Running time	up to several hours
Max. Reynolds number/m	480 million
Drive motor	94 MW
Fan speed	up to 600 rpm
LN_2 tank volume	946 m^3

Other Cryogenic Tunnels

We have discussed 15 cryogenic tunnels in this survey paper. There are other cryogenic tunnels we did not discuss. There have been some cryogenic tunnel projects started and then abandoned. These include the 1 ft and 4 ft cryogenic blowdown tunnels at the Douglas Company.[27]

There have been some special purpose cryogenic tunnels built, used, and retired after completing their work. In this category is the low-speed cryogenic tunnel built at Langley in 1971-72. In addition, we also built a small cryogenic tunnel at Langley in the early 1980's to study liquid nitrogen injection and evaporation.

Other cryogenic tunnels, such as the Cryogenic Isentropic Light Piston Tunnel at Cranfield,[28] still exist but are no longer used.

Our colleagues in the USSR and China undoubtedly have built cryogenic tunnels. Reference 29 describes a 2.4 x 2.4 m transonic cryogenic tunnel under study by Pan and his colleagues in China. However, we have no contact with these activities and remain mostly ignorant of their work.

Sources of Information

Reference 30 is a recent (September 1987) bibliography on cryogenic tunnels. The 467 papers cited in reference 30 cover most aspects of cryogenic tunnel development and use.

For current information on cryogenic tunnels we have the Cryo Newsletter published by the Experimental Techniques Branch. This informal quarterly newsletter is available from the Editor, Cryo Newsletter, Mail Stop 287, NASA Langley, Hampton, VA 23665-5225.

Final Remarks on Cryogenic Tunnels

Many cryogenic tunnels are in use. Some are large enough to let us test airfoils or aircraft models at full-scale Reynolds numbers.

Progress in building and using cryogenic tunnels has been slower than expected. Sometimes progress is slow because the designers and users of wind tunnels are not experts in cryogenic engineering. However, wind tunnel designers are beginning to learn how to design and install thermal insulation. Model builders are beginning to learn how to build models we can use the first time they are built. We are beginning to include good cryogenic engineering in our designs and operating procedures.

In spite of a few slow starts, some cryogenic tunnels run efficiently and safely on a routine production basis. Data from these tunnels is having a major impact on aerodynamic design. More cryogenic tunnels will come on line in the next year or so. Slightly further in the future the ETW will become operational.

The Japanese will build larger cryogenic tunnels. Sawada at NAL has proposed a 3 x 3 m transonic cryogenic tunnel capable of operating at 10 bars. Our friends at CARDC (China) will probably build their 2.4 x 2.4 intermittent cryogenic tunnel with stagnation pressures to 10 bars.

As with all previous advances in tunnel technology, cryogenic tunnels have been slow to find wide acceptance and application. We are always slow to accept radical changes in how things are done. However, momentum is gathering. The future for cryogenic tunnels is bright. The long awaited goal of testing at full-scale Reynolds number is at hand.

ADAPTIVE WALL TEST SECTIONS

The problem of wall interferences in wind tunnel testing remains despite considerable effort to eradicate it. Over the years, the wind tunnel community has used several well-known techniques to minimize wall interferences. Models are kept small compared with the test section size. Ventilated test sections are used to relieve transonic blockage. Linearized corrections are applied to the model data. Usually, all three techniques are used together in transonic testing. Unfortunately, we find these techniques are inadequate for high levels of accuracy we now demand from wind tunnel testing.

A solution to this dilemma exists. It involves using modern testing techniques which minimize wall interferences at source. (These modern techniques are a re-discovery of one of the first solutions to transonic wall interferences developed in the 1930s.) These techniques adapt the test section boundaries to free air streamline shapes, so the test section walls become invisible to the model. This is the **principle of wall streamlining**. Figure 9 shows the general case for a 3-D model. The test section boundaries follow an arbitrary free air streamtube round the model. (For simplicity we ignore the boundary layer growth on the test section boundaries.) Therefore, the free air flow field is split into a *real part* within the test section and an *imaginary part* round the test section. The imaginary flow field extends to infinity in all directions. The principle is simple but applying the principle is complex. The complexity arises from the need to adjust the test section boundaries for each test condition.

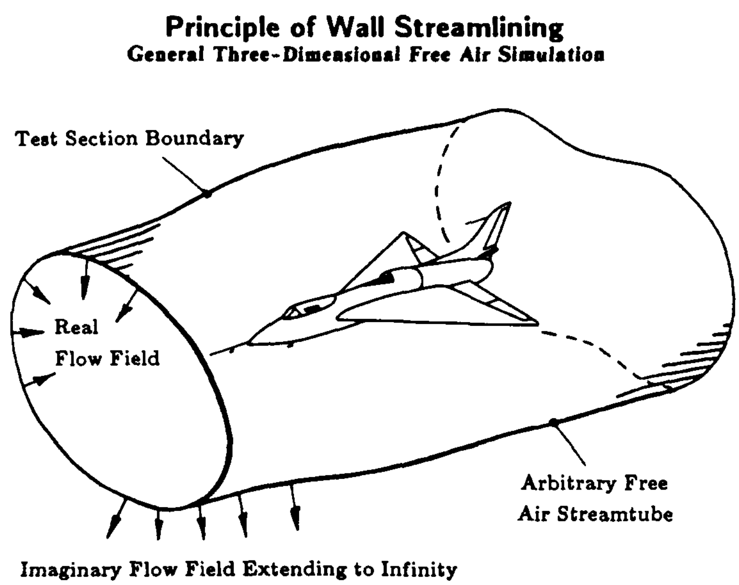

Fig. 9 - Principle of wall streamlining for general 3-D free air simulations.

We define a **streamlining criterion**[31,32] as the condition the adjustable boundaries must satisfy for the walls to be **streamlined/adapted.** (The term *adapted* is equivalent to the term *streamlined*, and we can refer to the *adjustable test section boundaries* as *adaptive walls.*) The streamlining criterion for free air simulations is straightforward. The adaptive walls must not support a local pressure imbalance between the real and imaginary parts of the flow field.

Advantages of Adaptive Walls

Other than the major benefit of minimizing wall interferences for free air simulations, adaptive wall test sections (AWTSs) offer other advantages. With wall interferences minimized, we are free to increase the size of the model for a given test section. Typically, we can double the test Reynolds number, perhaps allowing testing at full scale Reynolds numbers. Larger models are also important for high dynamic pressure tests and provide increased dimensions for more detailing and more volume for instrumentation. We can also expect simpler magnetic suspension of a model using an AWTS because the coils can be closer to the model.

With solid adaptive walls (called flexible walls), the test section boundaries are much smoother than with perforated walls. This smoothness reduces the tunnel drive power required for a given test condition with the model and test section size fixed. In addition, the removal of slots and holes reduces tunnel noise and turbulence levels improving flow quality. For intermittently operating tunnels, the removal of the plenum volume from the tunnel circuit reduces settling times and minimizes flow resonance.

Historical Overview

The modern adaptive wall testing techniques are a re-discovery of one of the first solutions to the problem of transonic wall interference. The National Physical Laboratory (NPL), UK built the first adaptive wall test section in 1938, under the direction of Dr. H. J. Gough.[33] They sought a solution to the problem of transonic blockage. Their research proved streamlining the flexible walls of an AWTS was a viable testing technique for high speed tunnels. They opted for minimum mechanical complexity in their AWTS by using only two flexible walls. Unfortunately, the absence of computers made wall streamlining a slow and labor intensive process. Sir G. I. Taylor developed the first wall adjustment procedure. His procedure was necessarily approximate to cut out the need for any calculations during the streamlining process. Nevertheless, NPL used flexible walled AWTSs into the early 1950s. They generated a large amount of 2- and 3-D transonic data,[34] which we are still uncovering in the literature.

The advent of ventilated test sections in 1946 provided a "simpler" approach to high speed testing, since the adjustments to the test section boundaries are passive. Consequently, ventilated walls superseded adaptive walls which actively control the test section boundaries. The AWTSs of NPL eventually became obsolete and disappeared.

After a 20-year lull, interest in AWTSs was rekindled in the early 1970s. Several researchers independently re-discovered the adaptive wall testing technique in the quest for improved data accuracy at transonic speeds.[32] Some advocated modifications of conventional ventilated test sections (the so-called variable porosity test section), while others opted for the NPL approach using flexible walled test sections.

This renewed interest has led to the establishing of various adaptive wall research groups around the world. Researchers have built many AWTSs of various designs for testing 2- and 3-D models. This development has even led to production type AWTSs.

Fallacies

During the development of any new technology, mistaken beliefs will arise. Adaptive wall technology has not escaped. A selection of mistaken beliefs follows:

The idea of AWTSs first appeared in 1972.
AWTSs will not work in large wind tunnels.
AWTSs will not work at transonic speeds.
AWTSs cannot streamline with sonic flow at the test section boundaries.
The testing technique is too complex to be practical.
The testing technique requires more computer power than conventional test sections.
Knowledge of the flow round the model is a prerequisite for wall streamlining.
Wall streamlining for each data point wastes too much tunnel time.
Operation of an AWTS requires expert knowledge.
2-D testing is trivial and the effects of the walls are not important.

We hope you will agree that these statements are indeed fallacies, after you read this survey.

AWTS Design

As mentioned in the historical overview, the renewed interest in AWTSs encompassed two approaches using ventilated or solid walls. We have observed many interesting designs during the modern era of AWTS development. In 2-D testing, only two walls need to be adaptable and researchers have tested both flexible wall and ventilated wall designs. The complexity of controlling a 3-D boundary has led to a variety of AWTS designs. Moreover, some approximation in the shape of the test section boundaries is inevitable. The magnitude of this approximation has been the subject of much research. The number of adaptive walls necessary in a 3-D AWTS is not simple to answer and must ultimately be a compromise. From practical considerations, the design of a 3-D AWTS must be a compromise between magnitude of residual interferences (after streamlining), hardware complexity, model accessibility and the existence of a rapid wall adjustment procedure. Table 16 shows the list of current AWTSs in use around the world, highlighting the variety of designs.

The vast research experience reported on 2- and 3-D testing with AWTSs[35] shows flexible walls to have distinct advantages over ventilated walls. These advantages are as follows:

a) Flexible walls can be rapidly streamlined.
b) Flexible walls provide more powerful adaptation control of the test section boundaries.
c) Flexible walls provide simple test section boundaries for adaptation measurements and residual interference assessment.
d) Flexible walls improve flow quality providing reduced interferences and reduced tunnel operating costs.

In 2-D testing, flexible walled test sections have operated with test section height to chord ratios of unity. In addition, we have recorded model normal force coefficients up to 1.54 with the walls streamlined. No ventilated AWTS, past or present, at Calspan, AEDC, or NASA Ames can match these conditions. The demonstrated 2-D capability of flexible walled test sections can be adequate for current production type testing, as shown later.

The old claim that ventilated AWTSs could be simply made from modified conventional ventilated test sections is no longer relevant. From AEDC and NASA Ames research,[36,37] we now know that substantial changes to a conventional ventilated test section are necessary to make it adaptive. Therefore, any update of an existing wind tunnel to adaptive wall status will involve the design of an AWTS insert. Any attempt to modify an existing test section would probably be much more difficult and involve too many compromises.

Researchers have investigated various numbers of adaptive walls in many AWTS designs for transonic 3-D testing. DFVLR used a nominally circular thick rubber tube in their DAM test section[38] with eight circumferential positioning jacks at each streamwise station for boundary control (see Figure 10). Similarly controlled, Technical University of Berlin (TU-Berlin) built an octagonal AWTS[39] with eight flexible walls sealed to one another by spring steel leaves (see Figure 11). AEDC has built the only transonic 3-D variable porosity AWTS[36] which has four adaptive walls and a square cross-section. Here, wall adaptation is by adjustment of the local porosity at each of the four perforated walls (see Figure 12). In addition, researchers have made 3-D tests in 2-D AWTSs at NASA Langley (see Figure 13), University of Southampton,[40] ONERA,[41] and TU-Berlin.[39] These 2-D AWTSs use only two flexible walls and have roughly square cross-sections.

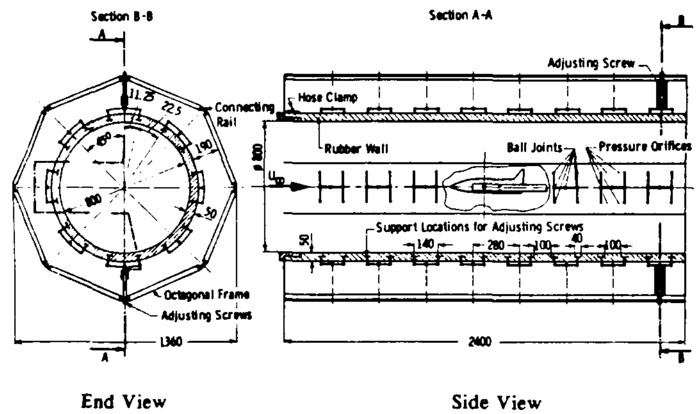

Fig. 10 - DFVLR Göttingen DAM rubber tube AWTS.

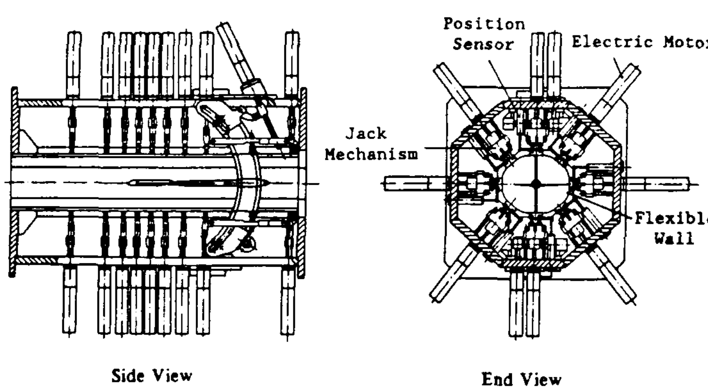

Fig. 11 - TU-Berlin octagonal AWTS with flexible walls.

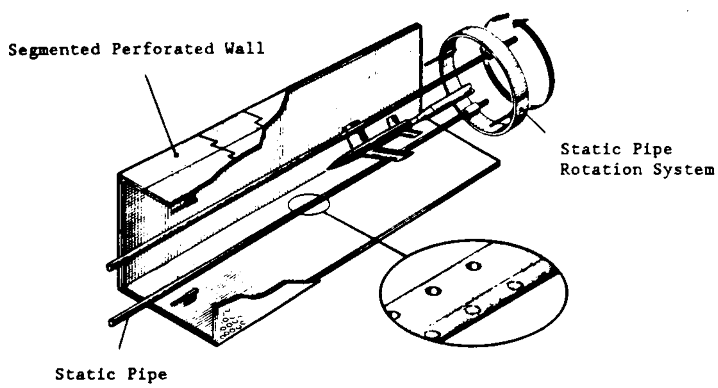

Fig. 12 - AEDC 1T Tunnel AWTS.

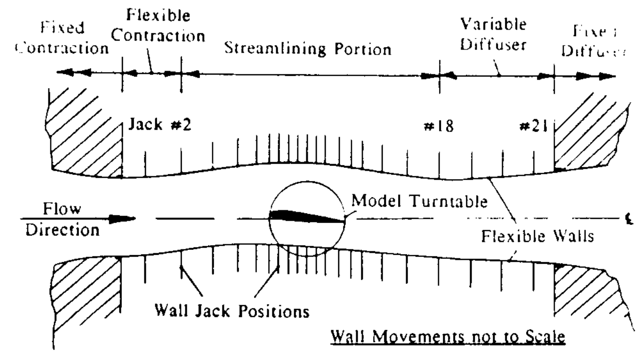

Fig. 13 - NASA Langley 0.3-m TCT flexible walled AWTS.

Experience with 3-D testing in AWTS is not as broad as we would like. Nevertheless, there are strong indications the simpler the AWTS the better the system. Simplicity reduces hardware complexity, gives better model access, and simplifies the assessment of residual interferences. We see no major disadvantages, but we need more research to confirm this. The development of 3-D adaptive wall testing techniques will continue to emphasize the trade-off between boundary adjustments and residual interference corrections. The outcome of this trade-off will effect the AWTS design.

We believe solid flexible walls offer the best approach to use of adaptive wall technologies in 2- and 3-D testing. Of the 14 high speed AWTSs operational worldwide, all but 2 use flexible walls.

Operational Experience with AWTSs

We direct operational experience with AWTS towards the following goals:

Minimization of time attributed to wall streamlining.
Examination of the operating envelope.
Establishment of an operating system for production-type testing.

Since 1975, researchers have made inroads into the time involved in wall streamlining, particularly with flexible walled AWTSs. A major part of this progress has been the development of rapid wall adjustment procedures for flexible walled AWTSs. (The term *rapid* refers to minimization of the number of iterations in the streamlining process.) For 2-D testing, the method of Judd, Goodyer, and Wolf[42,43] (University of Southampton, UK) is now well established for reasons of speed, accuracy, simplicity (we can easily use the method on any mini-computer), and adaptability to general use with flexible walled AWTSs. For 3-D testing, the methods of Wedemeyer/Lamarche[44] (Von Karman Institute, Belgium) and Rebstock[45] (TU-Berlin) show promise in speed and accuracy. Nevertheless, we require more evaluation of these methods before we can regard them as well established.

Other time-saving features of modern AWTSs are computer controlled movement of the adaptive walls and automated acquisition of wall data. However, for the tunnel user to benefit from the full potential of these time-saving features, we require a well defined streamlining criterion. This criterion optimizes the streamlining procedure. We find it necessary to compromise the streamlining criterion, described earlier, to allow for tunnel measurement accuracies. For 2-D testing, AWTSs at ONERA/CERT and TU-Berlin use the condition of insignificant wall adjustments and model flow changes. We prefer the condition of residual wall interferences reduced below acceptable minima used at the University of Southampton[32] and NASA Langley.[46] The acceptable minima are Induced $\alpha < 0.015°$; Induced camber $< 0.07°$; Induced velocity C_p error < 0.007. Unfortunately, we do not yet have a well defined streamlining criterion for 3-D testing. However, we find the net result of these time-saving features is an acceptable time attributed to 2-D wall streamlining, on the order of less than 2 minutes.

The examination of AWTS operating envelopes involves both hardware and software aspects of the AWTS control system. We show the streamlining procedure for any AWTS in Figure 14. The procedure involves an interaction between the tunnel hardware and the software. The hardware provides wall pressure data and wall adjustments as requested by the software. The software for analysis of the wall data contains the wall adjustment procedure and assessment of the wall streamlining quality. We base this quality on the free air streamlining criterion described earlier.

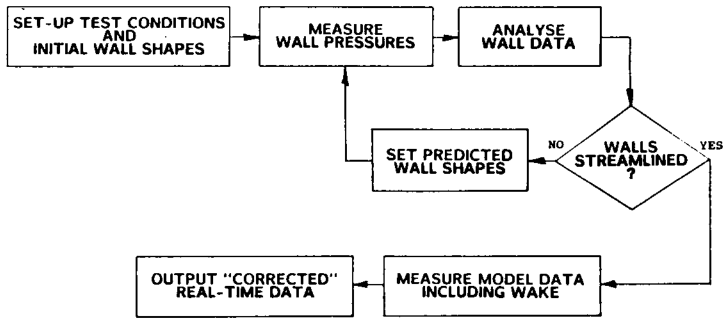

Fig. 14 - Streamlining procedure for each data point.

Good AWTS design should remove wall adjustment problems[32,46] (but we have yet to achieve this idyllic situation in any AWTS). Then only software limitations will restrict the operating envelope. At present, we can experience software limitations because we use linearized theory in the wall adaptation procedures. Since sonic flow on the flexible walls invalidates the procedures, we must restrict the free stream Mach depending on the model size compared with the test section dimensions. However, for 2-D testing, a wall adjustment procedure has been successfully developed based on Judd's method for 2-D testing at up to Mach 0.95.[47] (Software changes involve a more sophisticated representation of the imaginary part of the free air flow field, as discussed later.) Supersonic 2-D testing is also possible using wave theory to predict wall shapes. Software limitations in 3-D testing are not well defined since the software is in its development stage, but testing up to low supersonic is also possible.

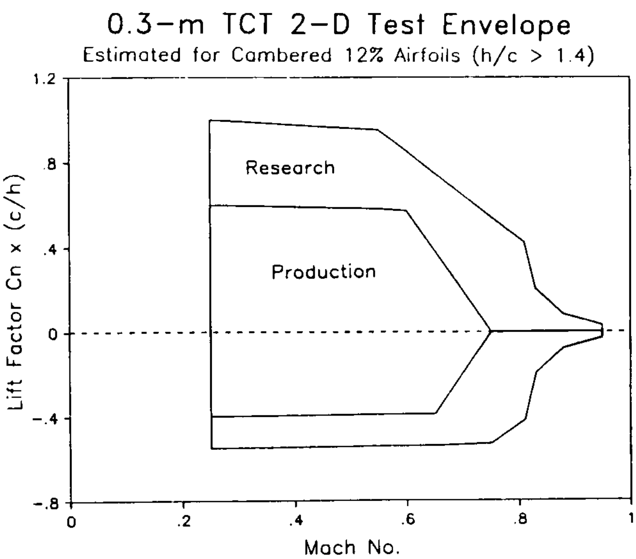

Fig. 15 - A model dependent test envelope for AWTS 2-D testing.

The establishment of an operating system for straightforward production-type testing is a prerequisite for general use of adaptive wall technology. If only experts can use this technology, then only specialist facilities can take advantage of the testing technique. Our research at Langley using the 0.3-m TCT[46] involves the first attempts to develop a production-type operating system. We are attempting to make invisible the complexities of the adaptive wall testing technique to the tunnel operators. Unfortunately, this difficult task is hampered by hardware shortcomings because of our unique application of an AWTS to a continuously operating cryogenic tunnel. Nevertheless, we have established an envelope for 2-D production-type testing (see Figure 15) based on model size and performance. This envelope is restrictive and we plan to expand it by hardware modifications.

Testing Results from AWTSs

There is a wealth of testing experience with AWTSs reported in the literature.[35] Validation testing forms a major part of this experience to determine data quality and limits to the operating envelope. In this section, we highlight the important observations to show the current State of the Art in adaptive wall research. We discuss 2-D and 3-D testing separately. We review data from various tunnels and where possible we include references to allow more detailed study of the results than necessary here. We present this data without prejudice. The data comes exclusively from flexible walled test sections because this design of AWTS is pacing the State of the Art.

2-D Testing Results from AWTSs

Effects of Wall Streamlining in 2-D Testing

Figure 16 shows the effects of adjusting the flexible walls of a 2-D AWTS on boundary interferences. With the flexible walls straight (simulating a conventional closed tunnel) the airfoil normal force coefficient, C_n, is typical of data with large wall interferences. There are considerable differences between the straight wall and streamlined wall values. This difference in C_n is a demonstration of classical lift interference induced by the test section boundaries, since the streamlined wall data are free of top and bottom wall interferences. Notice at the zero lift angle (near -4.6°) the flexible wall shape has no effect on model C_n. This shows the model blockage is small at zero lift. We took these data at a subsonic Mach number of 0.5. Notice the model experiences stall with the flexible wall streamlined. Meanwhile, with the flexible walls straight, the model C_n shows no stall up to the structural load limit of the model.

These data are for an advanced cambered airfoil tested in the NASA Langley 0.3-m TCT.[46] Notice the high C_n obtained during this test with the flexible walls streamlined. The maximum C_n of 1.54 is the highest ever achieved in any AWTS with the walls streamlined. The test section height to model chord ratio was a low 1.96 for this test.

Flexible Wall Effects on Model Data Through Stall at Transonic Speeds

M_∞ = 0.7, R_c = 12 million

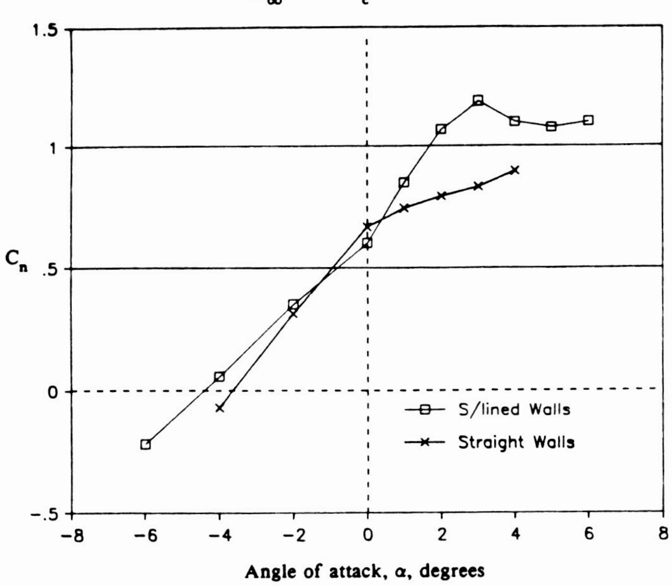

Fig. 17 - Effects of wall streamlining at Mach 0.7.

Flexible Wall Effects on Model Data Through Stall at Subsonic Speeds

M_∞ = 0.5, R_c = 3 million

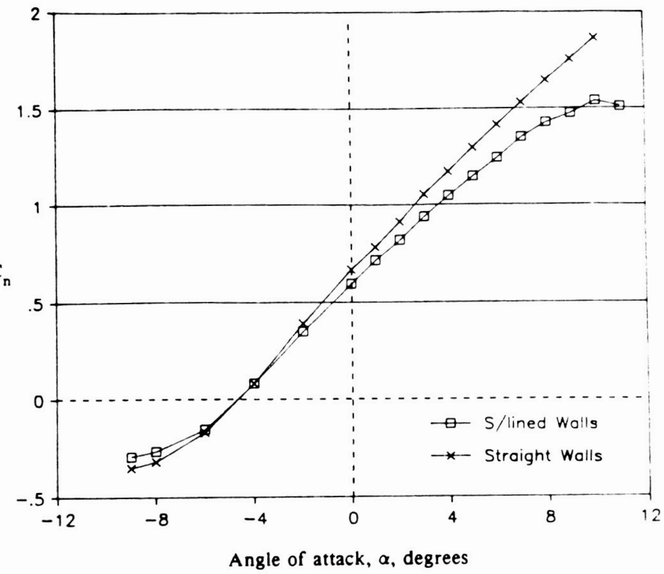

Fig. 16 - Effects of wall streamlining at Mach 0.5.

TSWT Schlieren Pictures

NACA 0012-64 Airfoil : M_∞ = 0.7 ; α = 4°

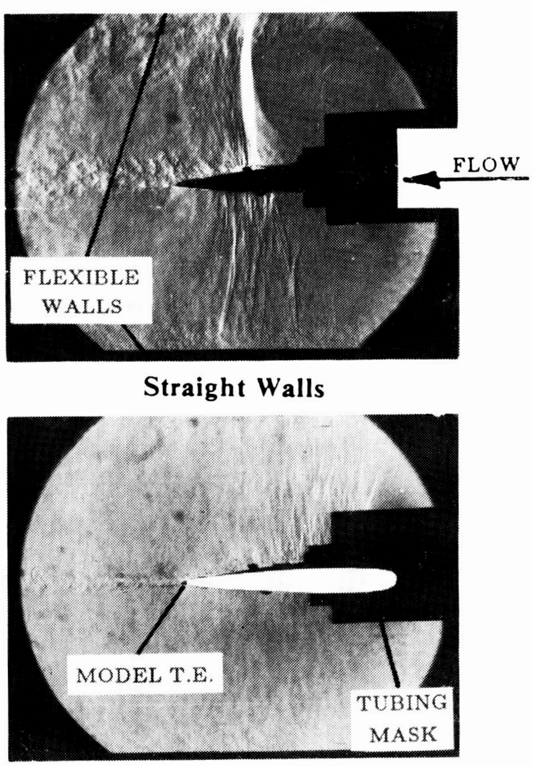

Streamlined Walls

Fig. 18 - Model flow changes with wall adaptation.

At transonic speeds the effects of adjusting the flexible walls are significantly different from the subsonic case. We show this difference in Figure 17. The onset of compressibility is an important factor in this difference. Notice how the lift interference changes sign at an angle of attack of about 0.5°. This is because of the phenomena of test section choking caused by increasing the model blockage. As we increase angle of attack, the model blockage increases due to the growth of shocks on the model surface. If we increase the angle of attack high enough, the flow channel above the model chokes causing significant wall interferences. We show this in Figure 18 with a schlieren picture from the Transonic Self-Streamlining Wind Tunnel (TSWT) at the University of Southampton, UK.[32]

By streamlining the flexible walls we can remove this choking and simulate an interference free flow field around the model. Sometimes, as shown here, the model shock changes position and reduces in strength. This causes a reduction in lift as for the subsonic case. However, the data in Figure 17 show that C_n increases at, for example, an angle of attack of 4°. This sign change is due to the use of different airfoils. (In the schlieren pictures the airfoil is symmetrical; the lift data are from a cambered airfoil.)

We highlight this point to show how unpredictable boundary interferences can be at transonic speeds. This unpredictability is because of the existence of non-linear flow field patches in the test section. Hence, the prediction of accurate corrections to the model data is very difficult using conventional correction techniques at transonic speeds.

Notice the straight and streamlined wall C_n data agree at two lifting angles of attack. While the values of C_n agree for these two cases, detailed pressure distributions do not agree. Interestingly, the zero lift angles do not agree for the two data sets. This shows that the model blockage is not small with the flexible walls set straight. At some higher Mach number the test section (with straight walls) will completely choke making the setting of higher Mach numbers impossible. However, streamlining the flexible walls removes this choking effect and allows us to test at higher Mach numbers.

Assessment of Residual Wall Interferences in 2-D Testing

The claim that 2-D AWTS data are free of wall interferences requires some qualification. We have made many validation tests on well known airfoils to assess the quality of free air simulations in AWTSs. Many published data comparisons show AWTS data matching "interference free" data.[5]

At Langley, we tried an alternative approach. We made an independent assessment of the residual interferences (we make a real time assessment to determine if the walls are streamlined) in the 0.3-m TCT with an AWTS using the NASA Langley Wall Interference Assessment/Correction (WIAC) procedures.[48] Figure 19 shows a plot of model lift coefficient, C_L, versus angle of attack which is an extract from this work. This plot shows how well AWTS data for two different size NACA 0012 airfoils compare to a theoretical prediction of the free air result, before and after correction for residual interferences. The corrections to the AWTS data are small and appear unnecessary for this case at Mach 0.6.

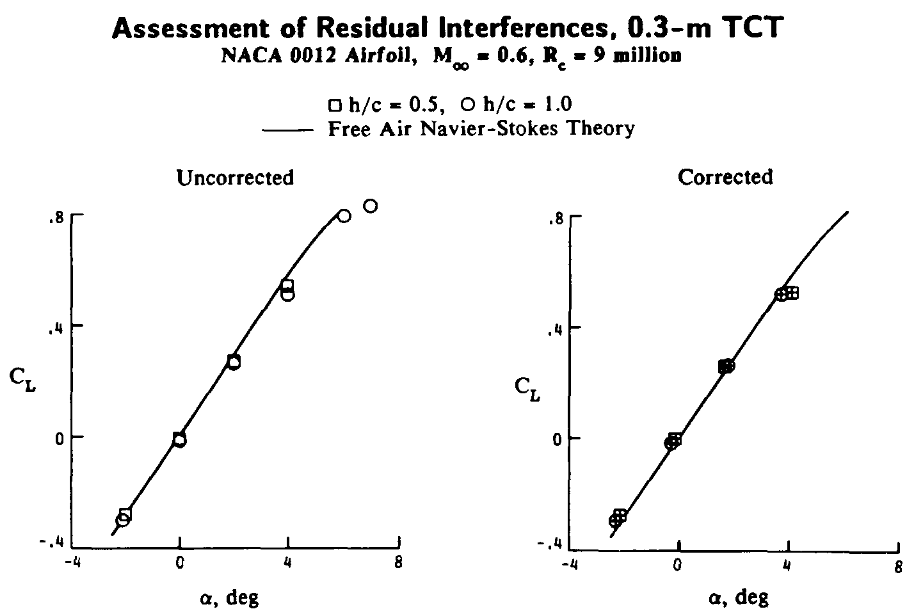

Fig. 19 - Comparison of NACA 0012 airfoil lift for two model chords with and without corrections according to the WIAC procedure.

ORIGINAL PAGE IS
OF POOR QUALITY

Also of significance is the agreement between AWTS data using different size models, one has a chord twice the other. The larger model has a test section height to chord ratio of 1.0. The comparison of model pressure distributions for the different chord airfoils is equally good. These and other[46] observations that the AWTS data are independent of model size further support the claim that the AWTS data are free of wall interferences.

2-D Testing with Sonic Flow at the Test Section Walls

Figure 20 shows wall streamlining for a 2-D airfoil in a fully choked test section is possible. The montage of real and imaginary flow fields comprises a schlieren picture of the test section flow at the airfoil. Shown with this picture are the outlines of the supercritical patches in the imaginary flow field outside the flexible walls. In the test section flow both airfoil shocks reach the flexible walls. The montage shows how well the flow fields match at the flexible wall interfaces to satisfy the free air streamlining criterion. This good match, particularly about the shock locations and sonic points, is an indication of good wall streamlining.

Researchers made this demonstration in TSWT at the University of Southampton during 1986.[47] The test section height to chord ratio for this test is 1.5. They used a modern Transonic Small Perturbation (TSP) code to calculate the imaginary flows. They found an uncomplicated procedure for wall streamlining. The wall adjustment procedure used here is a more sophisticated version of Judd's method, which includes TSP and wall boundary layer calculations.

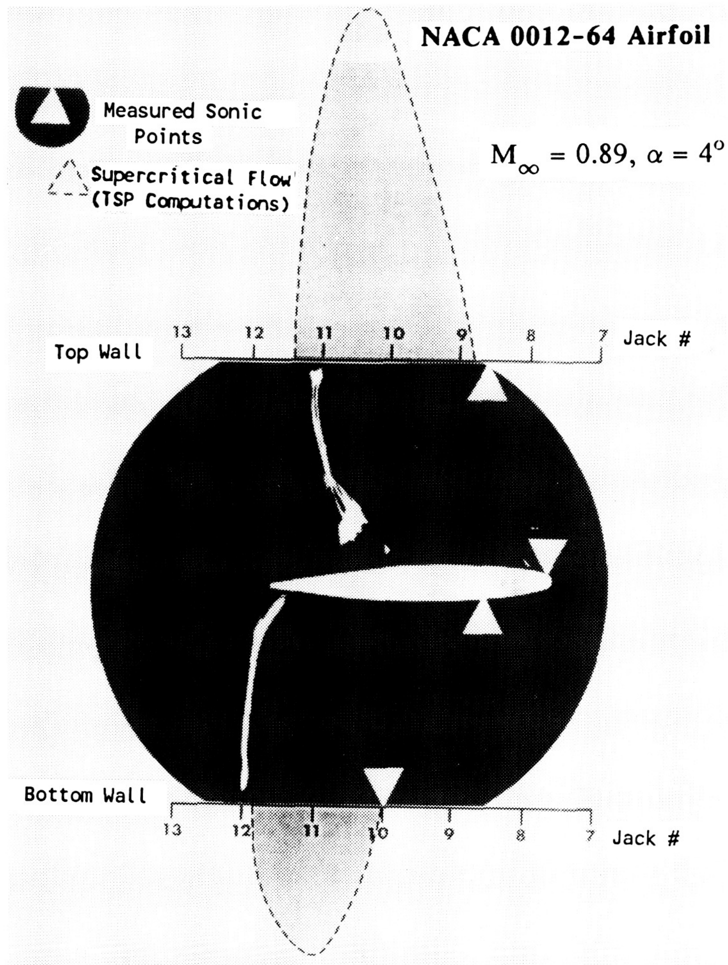

Fig. 20 - Montage of real and imaginary flow fields.

An important observation from these tests is the non-existence of shock reflections from the flexible wall. For some time skeptics considered the potential of shock reflections as a serious limit to Mach number. We now know this is not the case. Until the oblique bow shock appears ahead of the model near Mach 1.0, there cannot be any reflection problems. Even when an oblique shock appears, there is every indication that any reflections can be at least directed away from the model by a suitable wall curvature.

Effect of Compressibility on Flexible Wall Contours in 2-D Testing

So far, we have only looked at the airfoil data. It is also important to look at the wall contours required for streamlining, because we determine these contours without reference to the model. The wall contours should show expected aerodynamic trends if the wall adjustment procedure is working well.

A very graphic example of aerodynamic trends is the effect of compressibility on the wall contours. The plot in Figure 21 shows TSWT wall contours for two Mach numbers, one subsonic and one transonic.[32] The model, a NACA 0012-64 airfoil, was at a fixed angle of attack of about 4^o. The subsonic contours show lift induced upwash ahead of the model and a small model wake shown by the small movement apart of the walls downstream of the model. The transonic contours show minimal upwash ahead of the model because of loss of lift caused by a shock stall. In the region of the model, the walls move apart an amount equal to the airfoil thickness. Downstream of the model streams a large wake, shown by the large movement apart of the flexible walls. This large wake is due to shock induced flow separations on the model. The exaggerated wall deflection scale helps to amplify the effects of compressibility on the wall contours. We expected these effects. This finding adds to our confidence in the wall adjustment procedure of Judd et al.

These wall contours show the poor performance of the NACA 0012-64 airfoil at high speeds. This poor performance requires more severe flexible wall curvature for streamlining which could limit the test envelope. Better performing cambered airfoils demand less wall curvature at the same test conditions. So, the flexibility requirements of a wall are model dependent. We raise this point because it does complicate the AWTS design process.

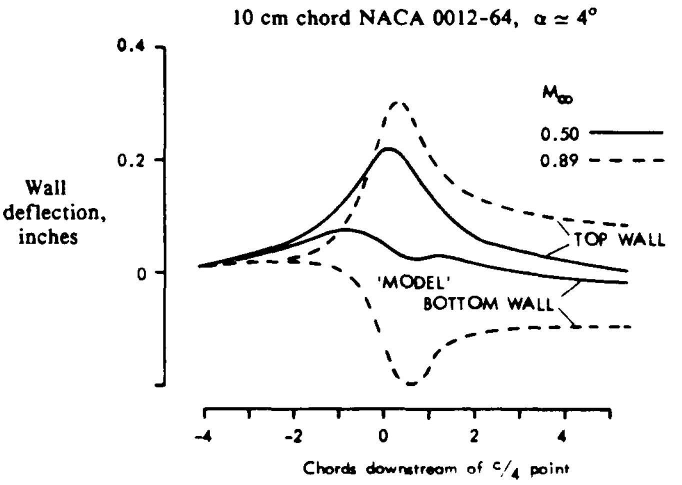

Fig. 21 - TSWT streamline wall contours at two Mach numbers.

Effect of Model Lift on Flexible Wall Contours in 2-D Testing

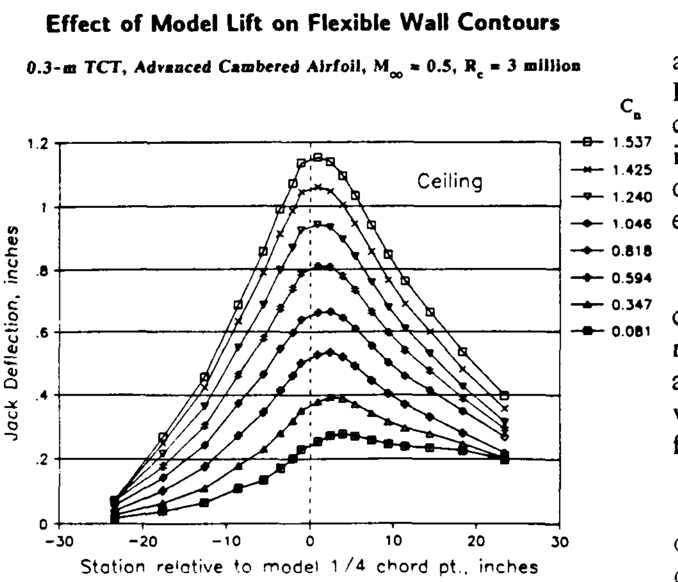

Fig. 22 - Family of streamline wall shapes with increasing model lift.

Figure 22 shows the upwash ahead of a lifting airfoil in the family of top wall (ceiling) contours. In this plot, we increase the model normal force coefficient, C_n, from near zero to 1.537. As C_n increases, so does the wall deflection. This increasing deflection is due to increasing model upwash and an expanding model wake associated with drag rise.

We again emphasize that we determine these contours experimentally without reference to the model. We show here data for a subsonic case to avoid complication of the wall contours associated with the onset of compressibility. Each wall contour fits into the family of shapes as expected.

This family of contours shows the usefulness of using streamlined wall contours for a lower angle of attack as initial contours for a higher angle of attack. The closer the initial wall contours are to the streamline shape, the quicker the streamlining procedure. This is because of reduced physical movement and reduced iterations within the streamlining procedure. In a series of tunnel tests over a range of angle of attack, the change in angle of attack between successive tests is probably up to 2°. This is equivalent to the interval between wall contours shown here. In this case, the choice of the streamlined contours for the last test as the initial contours for the next test is ideal.

Unfortunately, the effects of compressibility and operational requirements complicate this selection of initial contours. At transonic speeds, it is better to select streamline contours for a lower Mach number at the same angle of attack. We achieve operational flexibility by building a library of wall contours and, when necessary, calculating theoretical wall contours for a required set of test conditions.[46] So initial wall shapes are available for any sequence of test conditions.

2-D Testing Observations

There is a significant reduction of wall interferences by using AWTSs. We have found no problems with testing an airfoil through stall (no wall shape induced model hysteresis present). Different size models of the same section give the same results without correction, showing we have removed different levels of wall interferences in each case. Unfortunately, hardware limitations now restrict the test envelope for large airfoils (chords larger than 75 percent of test section height). Therefore, broader comparisons of data from different size models are not possible now.[46] Data repeatability is very good.

We have observed that the model wake in the 0.3-m TCT with an AWTS shows minimal spanwise variation. We speculate that the secondary flows at the airfoil-sidewall junction are small and boundary interferences are minimized. There is every indication the flow in the test section is an excellent simulation of a 2-D free air flow field.

Aerodynamic limits to free stream Mach number will occur if there are shock wave reflections on to the model. Researchers have made 2-D tests close to Mach 1.0[47] and some limited tests at Mach 1.2.[49] We have not yet encountered any fundamental limit to Mach number. However, the usefulness of 2-D testing in the supersonic regime may be only academic, providing experience leading to production supersonic 3-D testing.

The time attributed to wall streamlining should be small and is less than 2 minutes for a good operating system. Researchers have proposed some improvements to the wall adjustment procedure of Judd et al.[47] These improvements are for testing of large models at transonic speeds (when the wall slopes are not small) and for simpler selection of initial wall shapes. We have taken up to 50 data points in an 8-hour work shift. The most time consuming operation in our 0.3-m TCT with an AWTS[46] is the drag rake operation. Our experience shows production type testing is now possible with AWTSs.

3-D Testing Results from AWTSs

Effects of Wall Streamlining in 3-D Testing

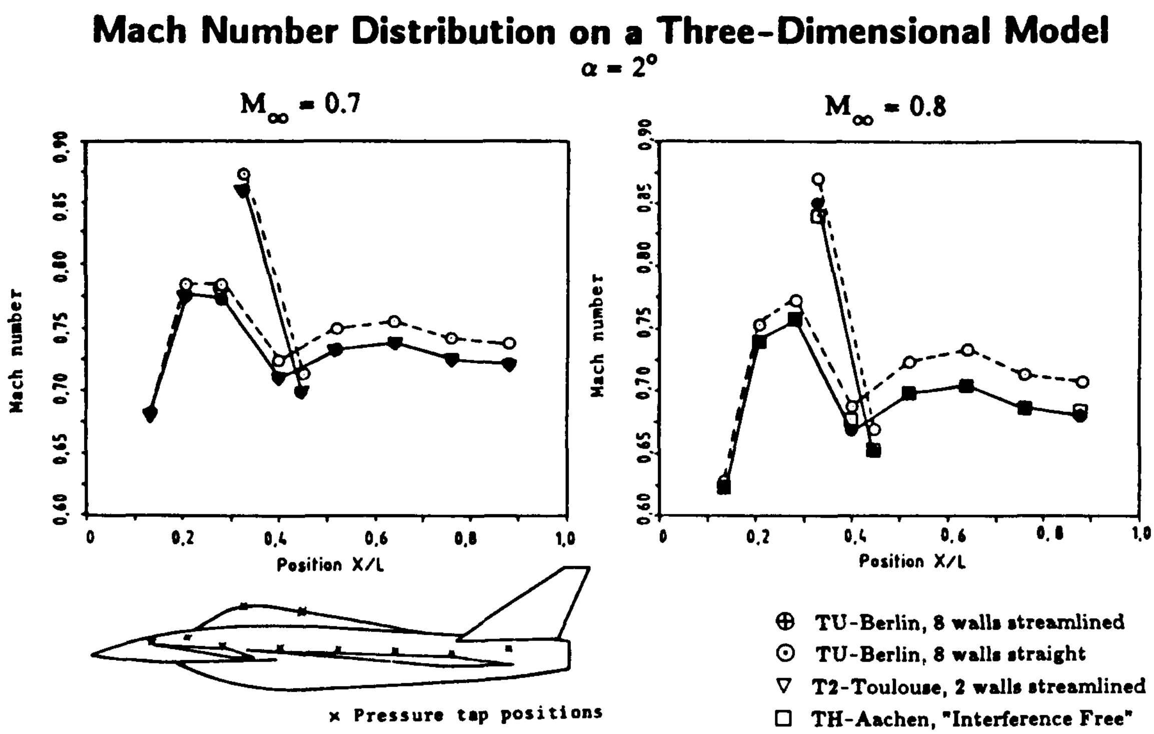

Fig. 23 - Mach number distributions on a 3-D canard model.

Figure 23 shows pressure data measured on a canard model of low aspect ratio (see Figure 24). Researchers have tested this model in several tunnels at free stream Mach numbers of 0.7 and 0.8. Stagnation conditions were ambient. There are two data sets from the TU-Berlin octagonal AWTS.[39] One set is with the eight flexible walls streamlined according to a 3-D wall adjustment procedure of Rebstock.[45] The other set is with the eight walls set straight. The two sets show the levels of interference removed by wall streamlining. Also shown is a data set from the ONERA/CERT T2 tunnel, which has a larger AWTS with two flexible walls.[50] For this data set, researchers streamlined the flexible walls according to a 3-D wall adjustment procedure of Wedemeyer and Lamarche.[44] We show the data from TH-Aachen as "interference free" data, since the model was very small in this tunnel. The comparison between the streamlined wall data and the "interference free" data is excellent. This observation is good for the adaptive wall testing technique but also shows that two flexible walls may be as good as eight.

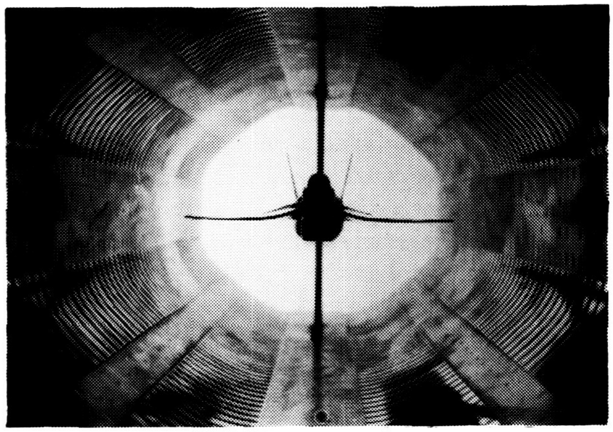

Fig. 24 - Canard model mounted in the TU-Berlin octagonal AWTS.

Figure 25 shows a comparison of lift coefficient, C_L, and drag coefficient, C_D, for the same canard model as before. We compare data sets from the octagonal AWTS and the T2 AWTS with streamlined walls, together with reference data from TH-Aachen.

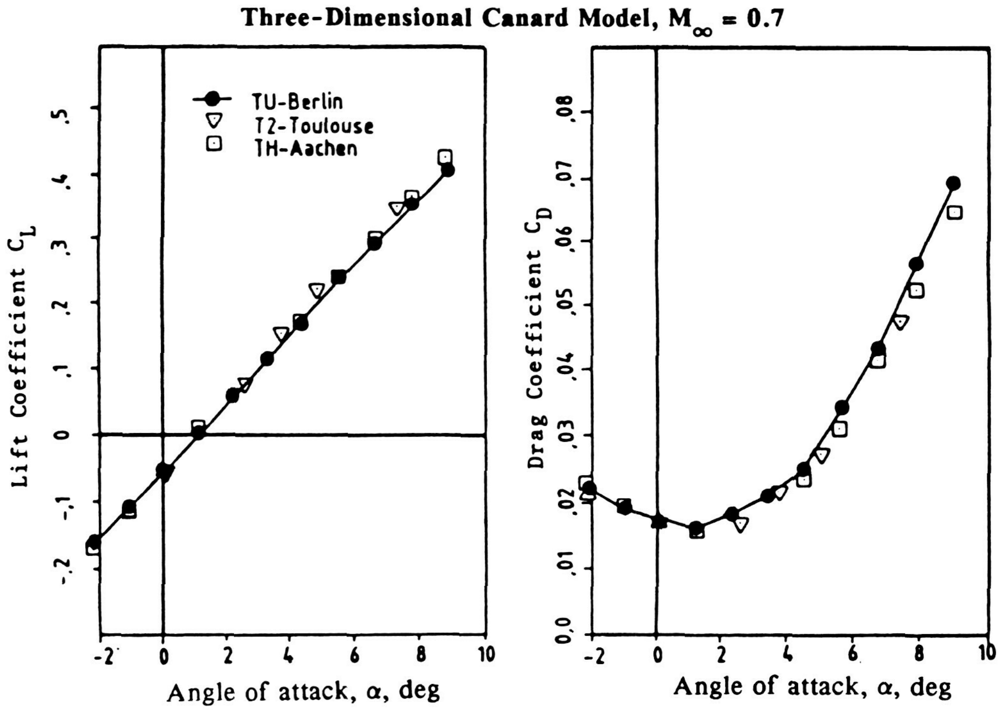

Fig. 25 - Comparison of force data from three tests of the canard model.

The comparison of lift coefficient is reasonable. The T2 data agrees slightly better with the reference data at the higher angles of attack. However, the differences are small and the data from the two AWTS show minimal boundary interferences. This is despite the fact neither AWTS is able to provide perfect control of its test section boundaries in three-dimensions. Model size and type probably have a strong influence on this, since real-time data on 3-D models in an AWTS should require residual corrections. Unfortunately, no publicized AWTS tests have had severe enough test conditions to leave significant residual interferences in the model data, after wall streamlining.

We find a similar comparison to the drag data. Again the T2 data agree slightly better with the reference data at the higher αs. We can explain this weak tendency for the TU-Berlin data to differ at high α as a blockage effect because of the large relative size of the model in the octagonal AWTS (see Figure 24). The nominal blockage of the canard model is 1.3 percent in the octagonal AWTS (the largest reported blockage in a 3-D AWTS test with a non-axisymmetric model) and 0.18 percent in the T2 AWTS.

Flexible Wall Contours for 3-D Tests

The flexible walls of the TU-Berlin octagonal AWTS are usually streamlined after two iterations starting from straight. We depict an example of the required wall shapes in Figure 26 for the top wall only. Notice the large wall deflections necessary downstream of the canard model. These deflections are necessary to accommodate the downwash generated by this high lift configuration.

Interestingly, researchers obtained similar streamlined wall shapes shown in Figure 27 in the ONERA/CERT T2 AWTS with just two flexible walls. They obtained these wall contours during tests of a lifting half model mounted on one sidewall of the AWTS.[41] The free stream Mach number was 0.6. The aerodynamically straight wall contours generate a constant Mach number distribution along the empty test section at Mach 0.6. We use these contours as a reference. They determined the streamlined wall contours by using the 3-D wall adjustment procedure of Wedemeyer and Lamarche.

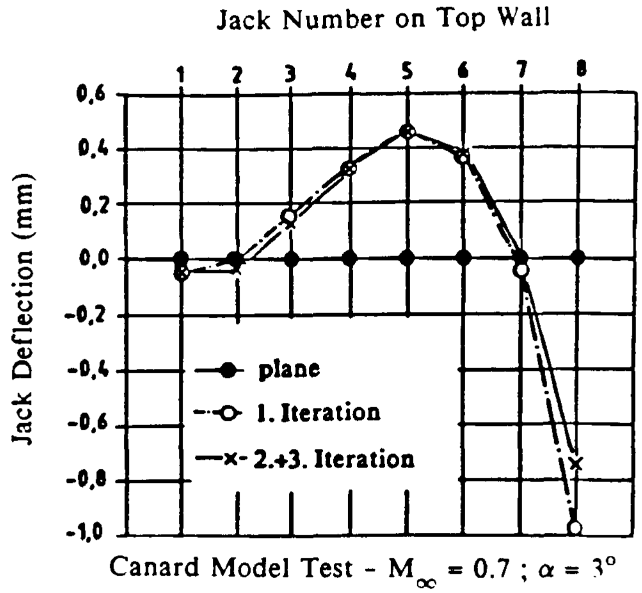

Fig. 26 - Convergence of the top wall contours during a typical 3-D test in the TU-Berlin octagonal AWTS.

For comparison, we also show wall shapes found using a 2-D wall adjustment procedure. There is a fundamental difference between 2-D and 3-D procedures. The 2-D procedure attempts the impossible, that is to remove 3-D wall interferences in a 2-D sense. Meanwhile, the 3-D procedure attempts to modify the 3-D wall interferences so they become correctable. This difference causes the prediction of different wall contours with the same test conditions and model in the tunnel.

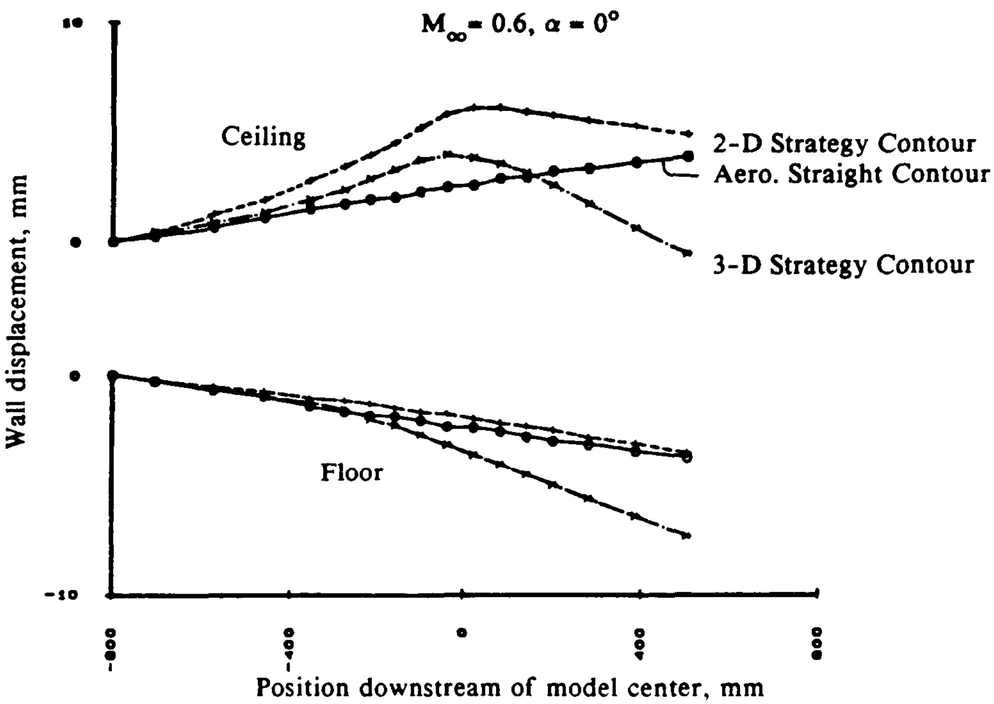

Fig. 27 - Floor and ceiling wall contours from the ONERA/CERT T2 Tunnel during 3-D tests using 2- and 3-D wall adjustment procedures.

From a designer's point of view, the general wall shapes for streamlining in a 3-D test pose some problems. The downstream movements of the flexible walls required for streamlining tend to be large compared with movements encountered in 2-D testing. This movement requirement will make necessary a more complicated fairing arrangement between the downstream end of the test section and the rigid tunnel circuit, if we are not to restrict the test envelope or model size.

Supersonic Tests in a 3-D AWTS

Figure 28 shows pressure distributions on a cone-cylinder at Mach 1.2. DFVLR Göttingen made these tests in their rubber tube DAM AWTS.[38] We show two pressure distributions, one before wall adaptation and one after. This adaptation involved the calculation of adjustments to the rubber tube at one streamwise location to absorb expansion and compression waves.

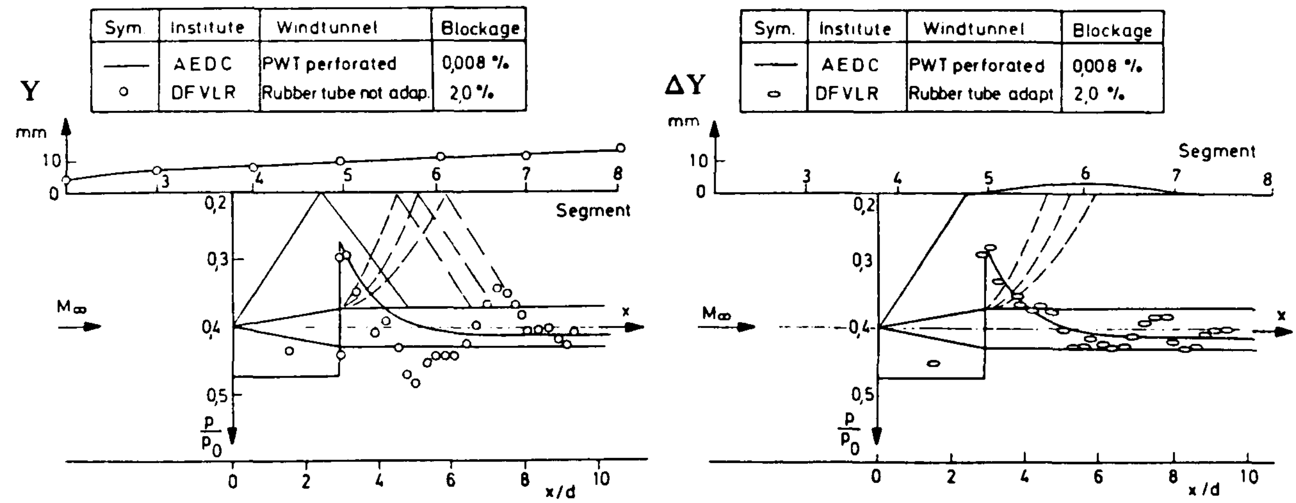

C_p distribution before adaptation

C_p distribution after adaptation
Wall displacement, $\Delta Y = 3.5$ mm at 6th segment

Fig. 28 - 3-D Supersonic Tests in the DFVLR DAM rubber tube AWTS.

Shown with the DFVLR data is reference data from the AEDC PWT tunnel with a very small model. Hence, we can consider this data as "interference free." With the rubber tube straight, there is a reflection of the model bow shock onto the model at $x/d = 5.0$. We see this interference as a local pressure rise on the model. Wall adaptation significantly reduces this interference.

The researchers at DFVLR did not design this AWTS for supersonic testing. Therefore, finer wall adjustments would only be possible if the wall jacks were closer together. However, a remarkable reduction of wall interference is possible with coarse wall adaptation. There would seem to be no fundamental limit to the use of flexible walls at supersonic speeds.

3-D Testing Observations

Reported validation tests[35] support the claim of minimized wall interferences in 3-D testing using an AWTS. However, the interferences present before any wall adaptation are already small because of the low blockage of 3-D models. This observation highlights the need for improved accuracy in the wall streamlining and makes operation of an AWTS more prone to measurement error. We can improve this situation by using more accurate instrumentation to refine our definition of the test section boundary conditions. Alternatively, we can scale up the complete test section and maintain the same measurement accuracy. In addition, we can increase the model disturbances in the test section by using larger models or testing only at high speeds. However, further research is necessary to determine just how large a 3-D model we can successfully test.

There are limits to the claim of minimized wall interferences in 3-D testing. The most significant limit found in all present AWTSs is flexible wall movement capabilities. This hardware limit severely restricts model lift. In addition, the cross-sectional dimensions of current AWTSs with the test section height roughly equal to the width unnecessarily restricts the size of non-axisymmetric lifting models. The only way to physically increase model blockage above the conventional 0.5 percent limit is to use low aspect ratio models. (We usually limit the model span to 65 percent of the test section width.) Thus, there is a need for special 3-D AWTSs of perhaps rectangular cross-section designed with a better understanding of the adaptive wall requirements.

The wall adjustment procedures for 3-D testing are still in a development stage. The need for faster and larger capacity mini-computers for real time 3-D computations is now satisfied. However, the total computing power required for 3-D tests in an AWTS is still equivalent to that required for using a conventional test section and computing off-line wall interference corrections. Several important questions about the wall adjustment procedures remain unanswered. How many wall pressure measurements are necessary to adequately define the test section boundaries? Also, where on the model is it best to minimize the wall interferences? We need further research to resolve these questions.

We have not found any aerodynamic limits to the minimization of boundary interferences. Preliminary tests at low supersonic speeds show we can use flexible walled AWTSs to remove oblique shock reflections onto the model. There is every indication routine testing at supersonic speeds is possible, although we have yet to show this.

Alas, the experience with 3-D testing still lags 2-D work. At present, no one uses an AWTS in production type 3-D testing. Researchers have made many 3-D validation tests over the years but have been unable to evaluate the operating envelope for 3-D AWTSs. So, many questions about 3-D testing in AWTSs remain unanswered.

The Future?

The development of AWTSs for 2-D testing has reached an important stage. Routine operation for current production 2-D testing envelopes is possible. We can test large models successfully to obtain significant increases in chord Reynolds number. The use of adaptive wall technologies in routine 2-D testing is a reality and the advantages are available to all.

The experience with 2-D testing has provided an important stepping stone to 3-D testing. Nevertheless, the progress of adaptive wall research in 3-D testing has not been very rapid. The reasons are not clear, but the availability of computers to carry out real-time 3-D flow computations may be a significant factor. Also, considerable 3-D AWTS research effort has gone into developing a wide range of complex AWTS designs, when it now appears the simpler 2-D design may well be adequate. (In hindsight, this effort appears unnecessary but the contribution to overall knowledge is nevertheless important.)

Several research centers are now pursuing the development of AWTSs for 3-D testing. Researchers need to probe the operating limits of the adaptive wall testing technique in 3-D testing. Then we can use the best methods to achieve specific test objectives and to demonstrate all the AWTS advantages. Only after these actions will there be any hope of removing the apparent unwillingness of the wind tunnel community to accept adaptive wall technologies. (This unwillingness is presumably linked to a phobia about the increased test section complexity associated with an AWTS.) Use of adaptive wall testing techniques can significantly raise the quality of wind tunnel data above current levels in several important areas. To achieve perfection, we must make full use of advanced technologies available to us.

TABLE 16. - ADAPTIVE WALL TEST SECTIONS CURRENTLY IN USE

Organization	Tunnel	X-Section (h x w) m	Length m	Approx. Max. Mach No.	Approx. Max R_c millions	Walls	Adaptation Control	Remarks
Arizona University ***	HLAT	0.51 Square	0.914	0.2		2 Arrays of Venetian Blinds 2 Solid	16 Panels of Vanes and a Variable Angle Nozzle	Issue 3
DFVLR ***	HKG	0.75 Square	2.40	>1.2		2 Flexible 2 Solid	? Jacks/Wall	
Genova University **	Low Defl. Cascade	0.2x0.05 Rectangular	1.58	>.9	1	2 Flexible 2 Solid	33 Jacks/Wall	
Genova University **	High Defl. Cascade	0.2x0.05 Rectangular	1.6	>.9	1	2 Flexible 2 Solid	13 Jacks-Ceiling 26 Jacks-Floor	
NASA Ames **	2x2 ft	0.61 Square	1.53	>.85	2	2 Slotted 2 Solid	32 PCCs/Wall	Issue 4
NASA Ames •	HRC-2	0.61x0.41 Rectangular	2.79	>.8	30	2 Flexible 2 Solid	7 Jacks/Wall	
NASA Langley **	0.3-m TCT	0.33 Square	1.417	>1.1	120	2 Flexible 2 Solid	18 Jacks/Wall	Issues 1/2/3/4/5
N P Univ. ** Xian, China	Low Speed	0.256x0.15 Rectangular	1.3	0.12	0.50	2 Flexible 2 Solid	19 Jacks/Wall	Issues 2/5
ONERA/CERT •	T.2	0.37x0.39 Rectangular	1.32	>1.0	30	2 Flexible 2 Solid	16 Jacks/Wall	Issue 2
ONERA •	S5Ch	0.3 Square	?	1.2		1 Multiplate 3 Solid	Transverse Sliding Plates	
RPI **	3x8	0.20x0.07 Rectangular	0.6	0.86		1 Flexible 3 Solid	6 Jacks	
RPI **	3x15	0.39x0.07 Rectangular	?	0.8		2 Flexible 2 Solid	?? Jacks/Wall	
Southampton University •	SSWT	0.152x0.305 Rectangular	0.697	0.1	0.38	2 Flexible 2 Solid	15 Jacks/Wall	40 ° Swept Wing Panel
Southampton University •	TSWT	0.15 Square	1.12	>1.0	2.5	2 Flexible 2 Solid	19 Jacks/Wall	Issue 1/3
Sverdrup *** Technology	AWAT	0.305x0.61 Rectangular	2.438	0.2		3 Multi-Flexible Slats 1 Solid	102 Jacks-Ceiling 51 Jacks/Sidewall	
Tech. Univ. Berlin •	I/II	0.15 Square	0.99	>1.0	2	2 Flexible 2 Solid	13 Jacks/Wall	
Tech. Univ. Berlin ***	III	0.15x0.18 Octagonal	0.83	>1.0		8 Flexible	78 Jacks Total	Issue 6
Umberto Nobile **	FWWT	0.2 Square	1.0	0.6	3.5	2 Flexible 2 Solid	18 Jacks/Wall	

** - 2D Capability
*** - 3D Capability
• - 2D and 3D Capability
PCC - Plenum Chamber Compartments

S.W.D. Wolf
November 1987

Note - The **Remarks** refer to issues of the **Adaptive Wall Newsletter** (published quarterly by the Experimental Techniques Branch, LaRC) in which we have published related articles.

MAGNETIC SUSPENSION AND BALANCE SYSTEMS

The first known wind tunnel Magnetic Suspension and Balance System (MSBS) was reported by ONERA in 1957. Since then 15 further systems have been constructed by 11 organizations around the world. Five systems are currently active and each will be reviewed briefly in this paper. Figure 29 highlights some milestones in MSBS development. The intense research activity in the 1960s faded due to the apparent difficulties and expense of building a large MSBS. Recent developments in the fields of large-scale applications of superconductors, advanced position and attitude sensors, and digital control systems have greatly enhanced the feasibility of a large MSBS. Research activity has therefore increased with two MSBSs operational at NASA Langley, two in England, one in Japan, and rising interest in other countries.

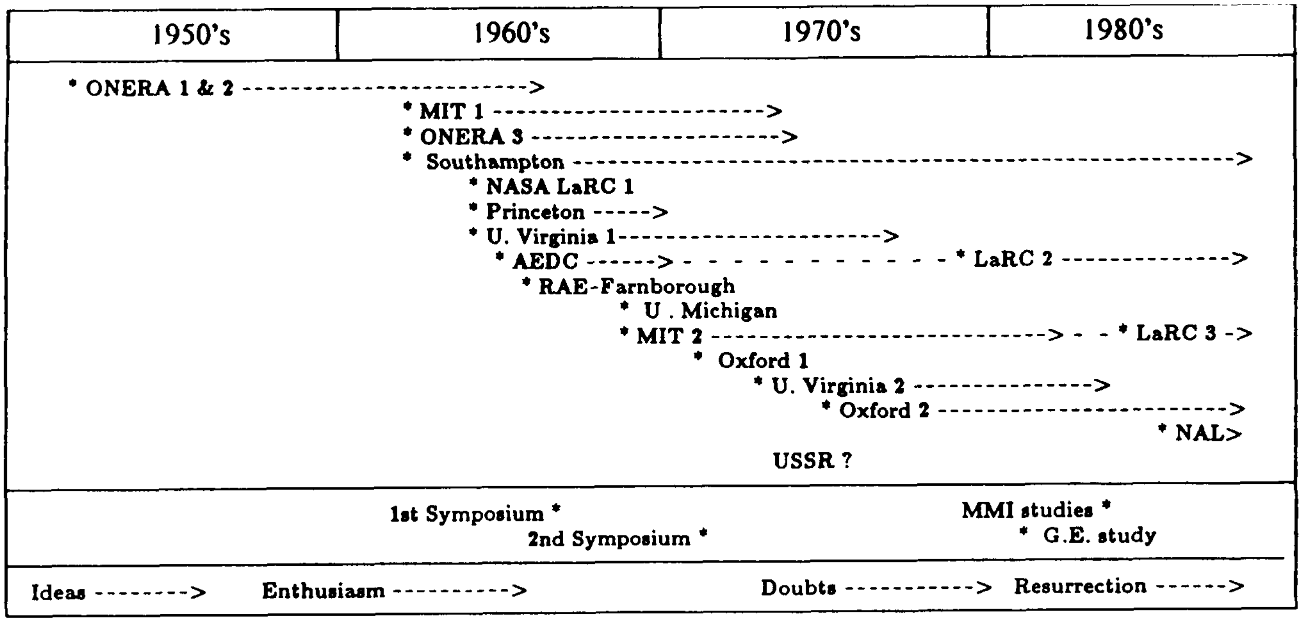

Fig. 29 - History of MSBS development.

Technical Background

The operating principles of MSBSs have been widely documented elsewhere and will not be repeated in this paper.[51] The principal attraction of MSBSs is, of course, the complete elimination of support interference. This problem, illustrated in Figure 30, can otherwise be particularly difficult in the transonic regime. Secondary benefits are the freedom to rapidly select model attitudes over a wide range and the possibility of more sophisticated and versatile dynamic testing than previously feasible.

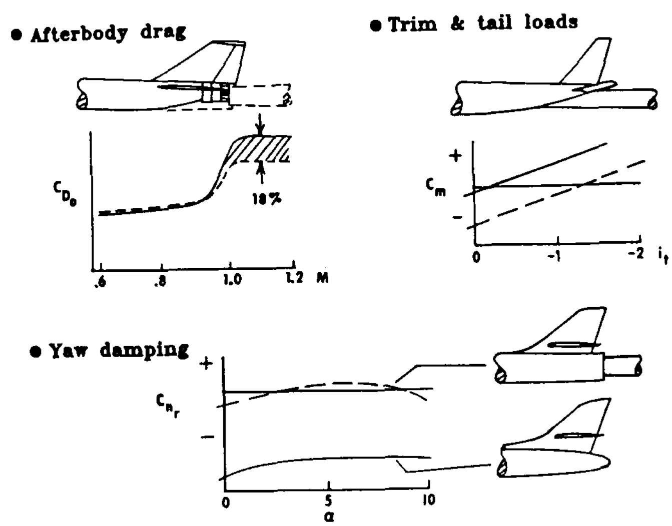

Fig. 30 - Examples of model support problems.

Current Magnetic Suspension and Balance Systems

United States
NASA Langley Research Center
13 inch MSBS

This system was originally built at the Arnold Engineering Development Center (AEDC) in the mid 1960s.[52] It was moved to NASA Langley in 1979 and has been progressively modified since then. In fact, of the original hardware, only the axial electromagnet and the support structure remain. The comments below relate to the present configuration.

Five electromagnets are arranged in a so-called V configuration, illustrated in Figure 31. The four vertical electromagnets are uncooled copper windings on laminated iron cores. The single water-cooled axial electromagnet is air cored. Model position and attitude is detected by an optical system based on solid-state, linear photodiode arrays. The control system is implemented with a PDP 11/73 minicomputer. Each electromagnet is fed from a bipolar thyristor power supply rated at 16kW. A low speed open circuit wind tunnel (maximum Mach 0.5) is installed. Figure 32 shows a schematic diagram of important hardware. Figure 33 shows a recent test in progress viewed from the control room.

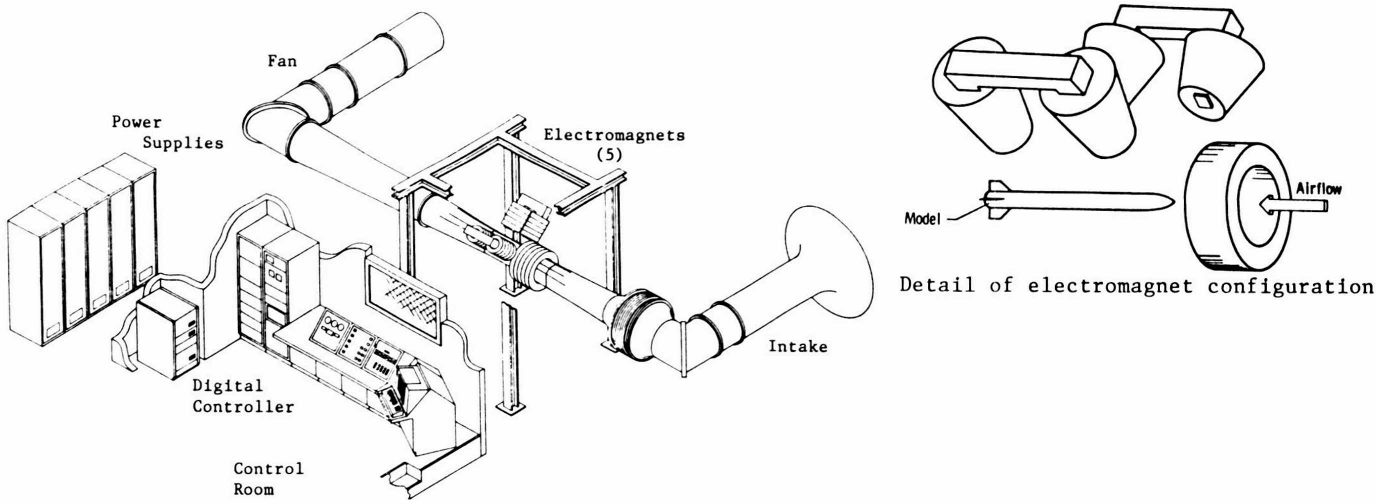

Fig. 31 - NASA Langley Research Center 13 inch MSBS.

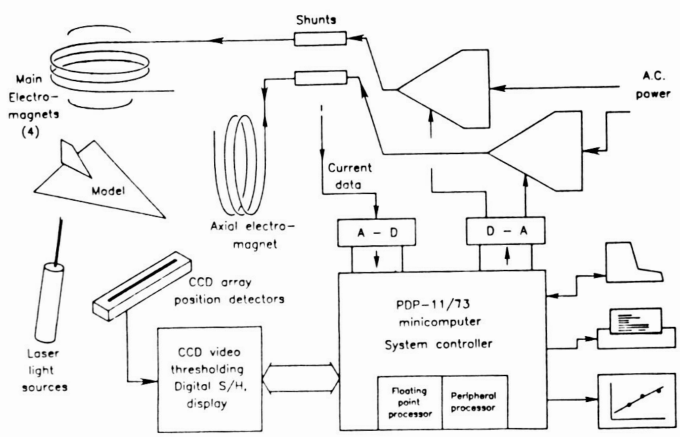

Fig. 32 - Schematic of 13 inch MSBS.

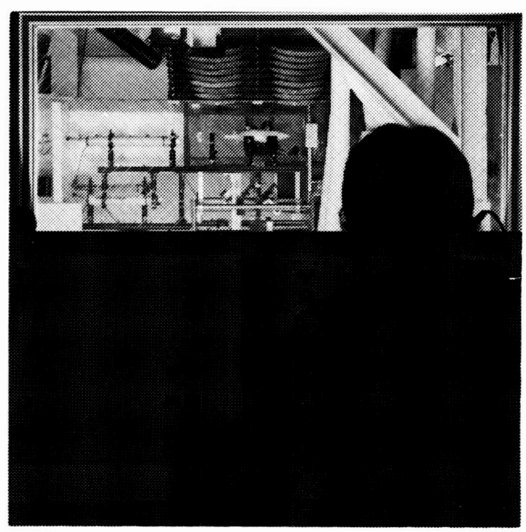

Fig. 33 - View from control room.

NASA Langley Research Center
6 inch MSBS

This system was built at the Massachusetts Institute of Technology in the late 1960s.[51] It was moved to NASA Langley and is operational in more or less its original form, shown in Figure 34. There are 16 separate water-cooled copper electromagnets supplied from a mix of thyristor, thyratron, and motor-generator power supplies. Six-component control is possible with an AC roll control scheme. Perhaps the most notable design feature is the use of an Electromagnetic Position (and attitude) Sensor (EPS). Upgrading of EPS electronics is under way. A digital controller has been ordered and replacement of the power supplies is anticipated soon.

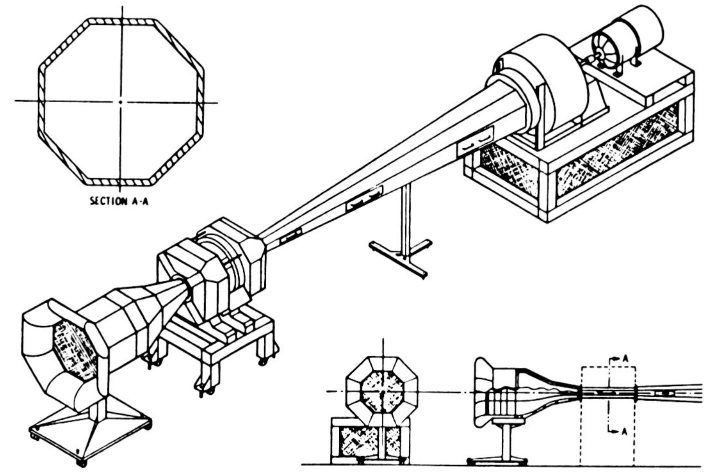

Fig. 34 - NASA Langley Research Center 6 inch MSBS.

Great Britain
University of Southampton
7 inch MSBS

Original construction of this system started in the mid 1960s. In its initial form it was used in low-speed, supersonic, and low-speed cryogenic wind tunnels. Extensive modifications were made in the early 1980s, including a fully symmetric electromagnet configuration, shown in Figure 35, and a digital controller.[53] The system is now installed in a purpose-built low-speed (M=0.3) wind tunnel. Electromagnets are uncooled copper windings, mostly using laminated iron cores, fed from bipolar transistor power supplies with a PDP 11/84 minicomputer based control system. An elaborate position sensing system, based on linear photodiode arrays, is presently installed to permit suspension up to 90° angle of attack. Previous achievements in high angle of attack suspension are shown in Figure 36.

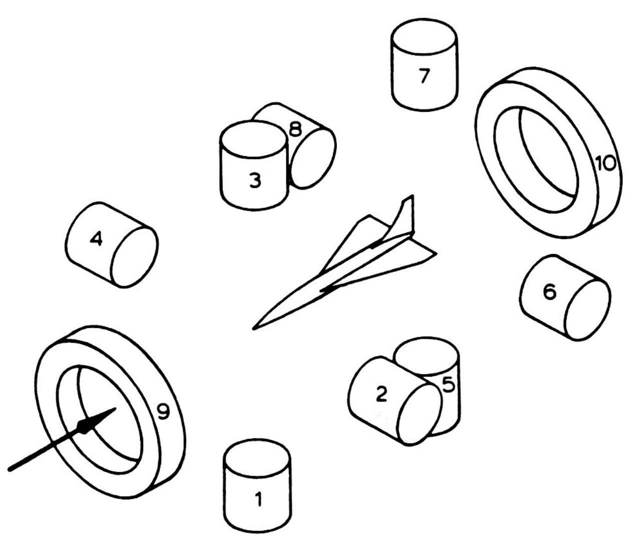

Fig. 35 - Southampton MSBS configuration.

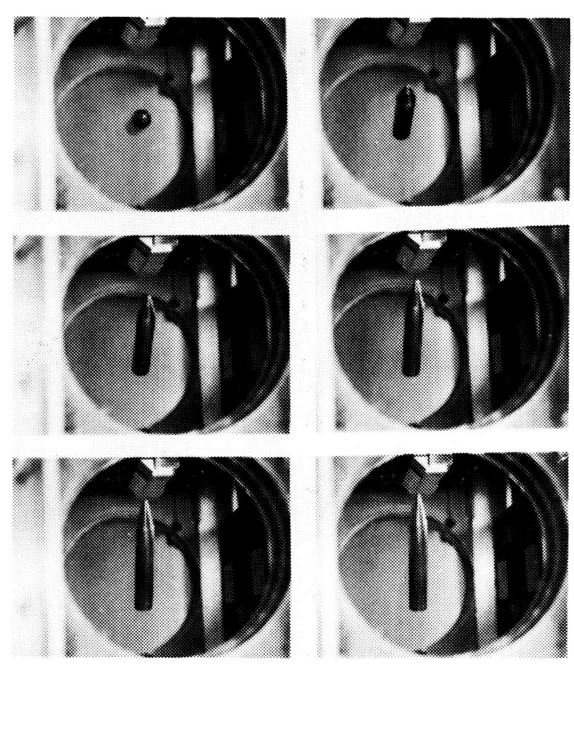

Fig. 36 - High angle of attack suspension.

ORIGINAL PAGE
BLACK AND WHITE PHOTOGRAPH

Oxford University
3 inch MSBS

For several years this MSBS has been in regular use measuring drag on small cone models in hypersonic low-density flows.[54] Figure 37 shows the system being prepared for a test. The system is simple in design, using eight water-cooled copper electromagnets for 3° of freedom control. Lateral motions are passively stabilized by special contoured pole pieces alongside the test section. An optical position sensing system and an analogue controller are used. Modifications are being studied to extend the angle of attack range for future testing.

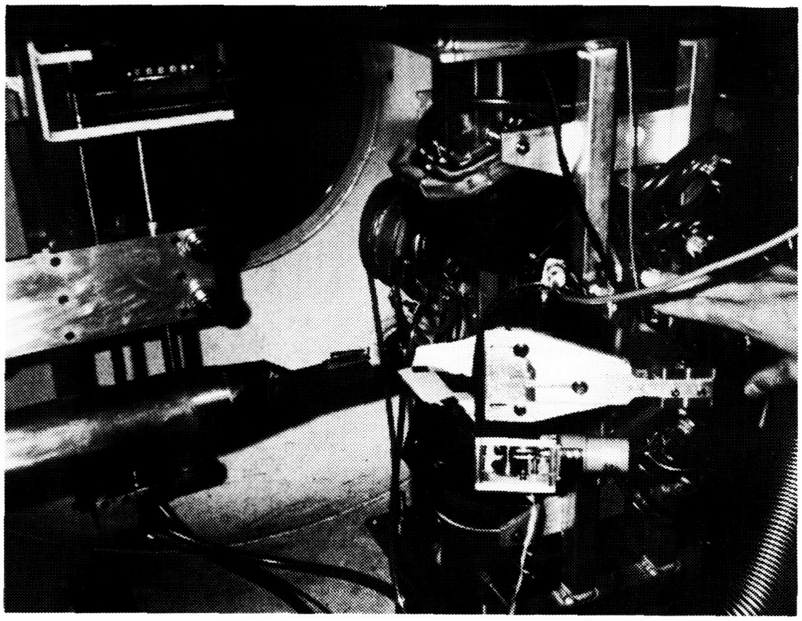

Fig. 37 - Oxford University MSBS.

Japan
National Aerospace Laboratory
4 inch MSBS

This system became operational in 1987. It is designed for 6° of freedom control but has apparently been used in 3° up to the present time. Ten electromagnets are arranged in a fairly symmetric configuration as illustrated in Figure 38. Model position and attitude sensing is carried out by a specially built camera assembly, comprising three linear photodiode arrays, illustrated in Figure 39. The camera operates in a passive mode, not requiring collimated light beams as used in other MSBSs. Current plans are to install the system in a small, transonic cryogenic wind tunnel in the near future.

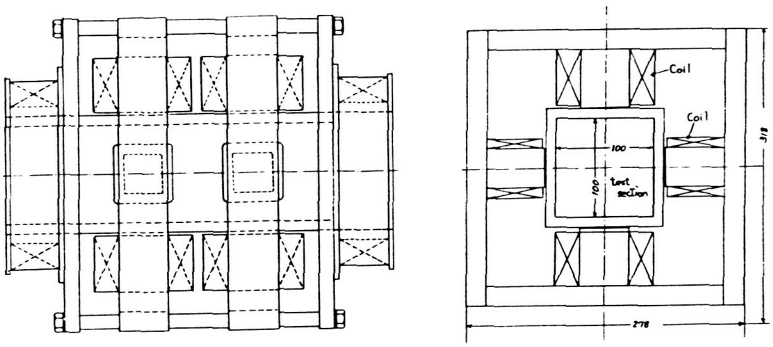

Fig. 38 - NAL MSBS configuration.

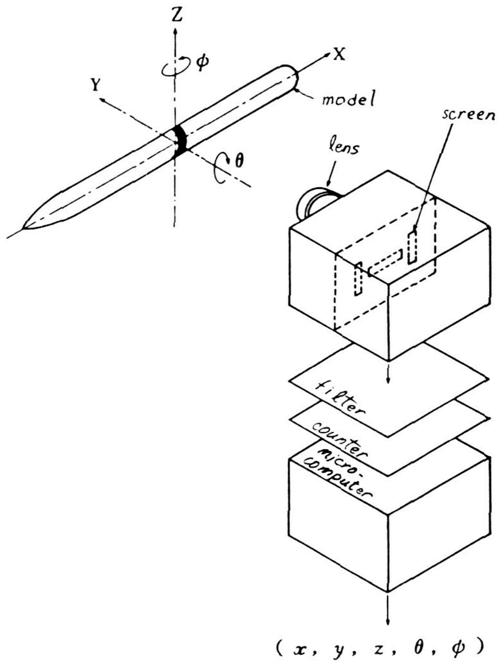

Fig. 39 - NAL position sensor.

Recent Aerodynamic Test Results

The NASA Langley 13 inch MSBS has been used for drag measurements on two laminar flow bodies of revolution (Hansen & Hoyt and Boltz). Preliminary testing of a family of slanted-base ogive cylinder models has been completed. Further tests will include sting interference assessment. The Southampton MSBS has also recently tested the Boltz body of revolution. High angle of attack tests of ogive-cylinder or similar models should begin at Southampton shortly. Hypersonic aerodynamic studies of cones at small angles of attack are planned at Oxford. The test program for the NAL MSBS is not known at this time. The NASA Langley 6 inch MSBS is devoted mainly to instrumentation development.

Large System Design

Three major design studies of large MSBSs have been completed.[55,56,57] Two of these are illustrated in Figure 40. All were targeted to an 8-foot, atmospheric, transonic tunnel. All studies concluded that the systems were technically feasible, though some care in design and specification is necessary to maintain reasonable costs. Latest studies indicate that the target system could be built for around $20 million. An industry survey revealed widespread support for continued MSBS development, focusing particularly on the transonic application.[58]

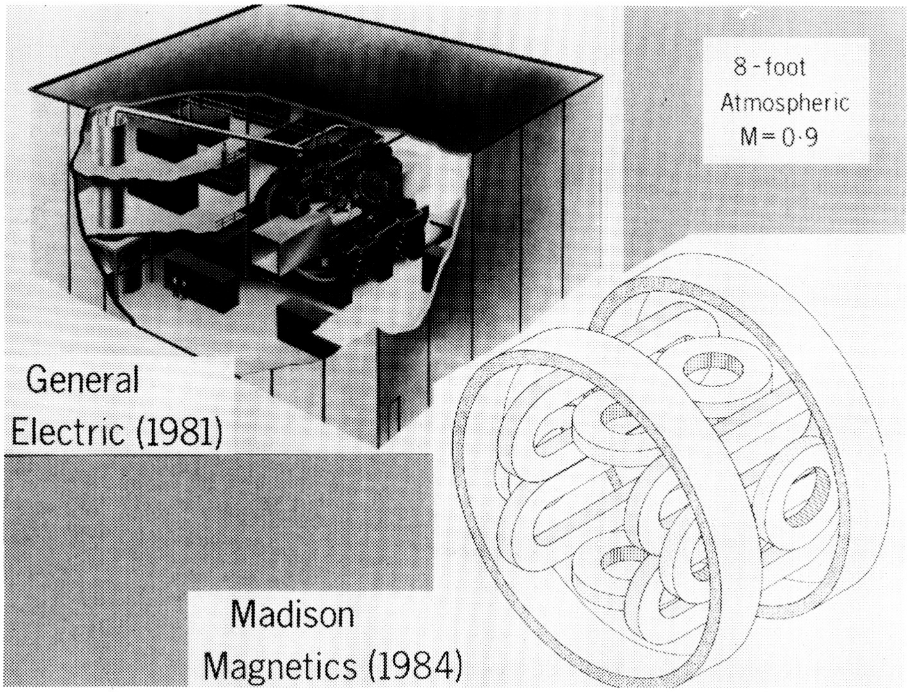

Fig. 40 - Large MSBS design studies.

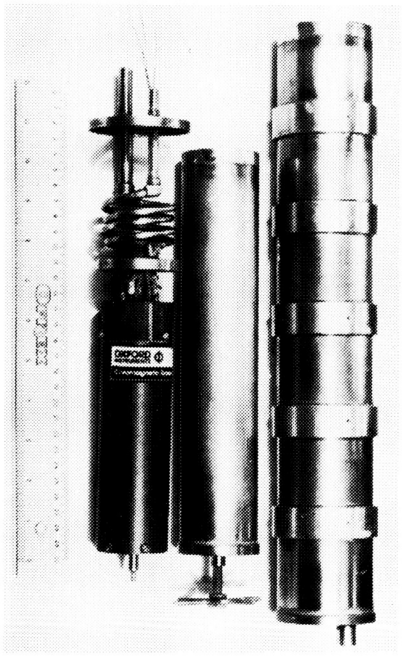

Fig. 41 - Superconducting solenoid model core.

New technology will continue to have an impact on the cost and usefulness of MSBSs. High angle of attack suspension methodology continues to advance at Southampton. Digital control systems are under widespread development.[59] The demonstration of a prototype superconducting solenoid model core, shown in Figure 41,[60] confirms the feasibility of this concept for large MSBSs where a significant reduction in electromagnet size can result from its use. New approaches to the problem of force and moment calibration are being pursued, including on-board strain-gage balance systems with data telemetry, illustrated in Figure 42.[61] High temperature superconductors may have a dramatic impact on the design and cost of a large MSBS, though it should be stressed that large MSBSs are feasible without these materials.

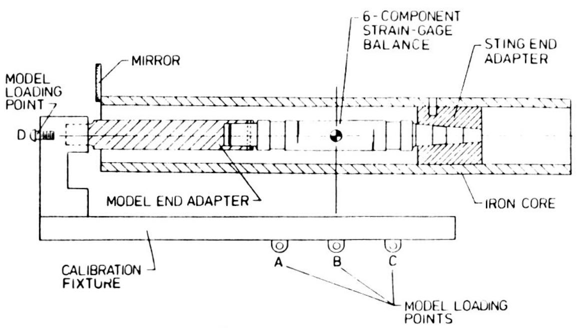

Fig. 42 - Internal strain-gage balance.

ORIGINAL PAGE
BLACK AND WHITE PHOTOGRAPH

CONCLUDING REMARKS

This survey paper covered **cryogenic wind tunnels, adaptive wall test sections,** and **magnetic suspension and balance systems** (MSBS). With a cryogenic tunnel researchers can test at flight Reynolds numbers. Having a test section with adaptive walls eliminates or greatly reduces wall interference effects. Using magnetic suspension of the model eliminates support interference effects.

Cryogenic tunnels are finding wide acceptance and use. The future for large cryogenic tunnels seems assured with the U.S. NTF and the KKK in operation and the ETW under final design.

Adaptive wall test sections are also finding wide acceptance and use. One remaining question is how complex the walls need to be for adaptation for 3-dimensional models. The next year or so will see this question resolved. Then we will see adaptive wall test sections in new wind tunnels as well as being retro-fitted in existing tunnels.

Magnetic suspension and balance systems are slower to find acceptance and application than either cryogenic tunnels or adaptive walls. One reason for this is the complexity of MSBS. Another is the limitation on size that existed before the development of so-called *ac* superconductors. The small systems now in use offer a glimpse of the tremendous potential of MSBS. The technology for building a large (8 foot or bigger) MSBS is now in hand. The building of large systems is just a matter of time.

The development of advanced test techniques is steadily moving forward. We now have the ability to test at flight Reynolds number free of both wall and support interference. The future for wind tunnel testing is bright.

REFERENCES

1. **Kilgore; Robert. A.; and Dress, David A.**: The Application of Cryogenics to High Reynolds Number Testing in Wind Tunnels. Part 1: Evolution, Theory, and Advantages. *Cryogenics*, vol. 24, pp. 395-402, 1984.

2. **Kilgore, Robert A.; and Dress, David A.**: The Application of Cryogenics to High Reynolds Number Testing in Wind Tunnels. Part 2: Development and Application of the Cryogenic Wind Tunnel Concept. *Cryogenics*, vol. 24, pp. 484-493, 1984.

3. **Dress, David A.; and Kilgore, Robert A.**: Cryogenic Wind Tunnels - a Global Perspective. *Cryogenics*, vol. 28, pp. 10-21, 1988.

4. **Law, R. D.**: Early Experiments in Using the Cryogenic Test Facility at RAE Bedford, UK. *ETW Cryogenic Technology Review Meeting*, Paper 8, NLR-Amsterdam, 1982.

5. **Goodyer, M. J.**: The 0.1m Subsonic Cryogenic Tunnel at the University of Southampton. NASA CR-145305, 1978.

6. **Kell, D. M.**: A Surface Flow Visualization Technique for Use in Cryogenic Wind Tunnels. Aeronautical Journal, vol. 82, November 1987, pp. 484-487.

7. **Goodyer, M. J.**: Engineering Changes to the 0.1m Cryogenic Wind Tunnel at Southampton University. NASA CR-172430, 1984.

8. **Owen, D.**: Development of a Mach Number Control System for Use With a Cryogenic Wind Tunnel. *Honours Project Report*, University of Southampton, UK, 1984.

9. **Britcher, C. P.; and Goodyer, M. J.**: The Southampton University Magnetic Suspension/Cryogenic Wind Tunnel Facility. *1st Int. Symp. on Cryogenic Wind Tunnels*, Paper 10, Southampton, UK, 1979.

10. **Tizard, J. A.; and Hartzuiker, J. P.**: The European Transonic Windtunnel Project ETW. AGARD R-722, Paper 12, 1985.

11. **Dor, J.-B.**: The T2 Cryogenic Induction Tunnel in Toulouse. AGARD R-722, Paper 9, 1985.

12. **Blanchard, A.; Delcourt, V.; and Plazanet, M.**: Problems Associated With Operations and Measurement in Cryogenic Wind Tunnels. Translation into English of "Problemes Lies Fonctionnement et aux Measures en Soufflerie Cryogenique." Rep. OA-13/5007-AYD DERAT-13/5007-DY, July 1981. NASA TM-88443, June 1986, 75 pp.

13. **Viehweger, G.**: The Kryo-Kanal-Köln project, KKK. AGARD R-722, Paper 11, 1985.

14. **Hefer, G.**: The Cryogenic Ludwieg Tube Tunnel at Göttingen. AGARD R-722, 1985, pp. 10-1 through 10-6.

15. **The Second Aerodynamics Division**: Construction and Performance of NAL Two-Dimensional Transonic Wind Tunnel. NAL TR-647T, 1982.

16. **Takashima, K.; Sawada, H.; Aoki, T.; and Kayaba, S.**: Trial Manufacture of NAL 0.1 m x 0.1 m Transonic Cryogenic Wind Tunnel. NAL TR-910, 1986.

17. **Adachi, T. et al**: Force and Vortex Shedding on a Circular Cylinder From Subcritical Up to Transcritical Reynolds Numbers. Bulletin of the JSME, vol. 28, no. 243, 1985.

18. **Clausing, A. M.; Clark, G. L.; and Mueller, M. H.**: The Cryogenic Heat Transfer Tunnel - A New Tool for Convective Research. *Winter Annual Meeting ASME*, San Francisco, California, 1978, pp. 73-78.

19. **Clausing, A. M.**: Experimental Studies of Forced, Natural and Combined Convective Heat Transfer at Cryogenic Temperatures. *1st International Symposium on Cryogenic Wind Tunnels*, Paper 24, Southampton, UK, April 3-5, 1979.

20. **Clausing, A. M.**: Advantages of a Cryogenic Environment for Experimental Investigations of Convective Heat Transfer. *International Journal of Heat and Mass Transfer*, vol. 25, no. 8, 1982, pp. 1255-1257.

21. **Mueller, M. H. et al**: Description of UIUC Cryogenic Wind Tunnel Including Pressure Distributions, Turbulence Measurements and Heat Transfer Data. *University of Illinois*, Tech. Rept. ME-TN-79-9180-1, 1979.

22. **Goodyer, M. J.; and Kilgore, R. A.**: High-Reynolds-Number Cryogenic Wind Tunnel. AIAA 72-995, 1972. Also, *AIAA Journal*, vol. 11, no. 5, 1973, pp. 613-619.

23. **Kilgore, Robert A. et al**: The Cryogenic Wind-Tunnel Concept for High Reynolds Number Testing. NASA TN-D-7762, 1974.

24. **Kilgore, Robert A.**: The NASA Langley 0.3-m Transonic Cryogenic Tunnel. AGARD R-722, Paper no. 13, 1985.

25. **Bruce, Walter E., Jr.**: The U.S. National Transonic Facility - I. AGARD R-722, Paper no. 14, 1985.

26. **Bruce, Walter E., Jr.**: The U.S. National Transonic Facility - II. AGARD R-722, Paper no. 15, 1985.

27. **Aldrich, J. F. L.**: Progress Report on the Douglas Four-Foot Cryogenic Wind Tunnel. *1st Int. Symp. on Cryogenic Wind Tunnels*, Paper no. 35, Southampton, UK, April 3-5, 1979.

28. **Stollery, J. L.; and Stalker, R. J.**: The Development and Use of Free Piston Wind Tunnels. *Proceedings of the 14th International Symposium on Shock Tubes and Waves*, Sydney, 1983, pp. 41-50.

29. **Pan, R.**: Cryogenic High Reynolds Number Transonic Wind Tunnel with Pre-cooled and Restricted Flow. Translated into English from Zhongguo Quiliu Dongli Xue (China), no. 2, pp. 76-92.

30. **Tuttle, Marie H.; Kilgore, Robert A.; and Cole, Karen L.**: Cryogenic Wind Tunnels - A Selected, Annotated Bibliography. NASA TM-4013, September 1987.

31. **Goodyer, M. J.**: The Self Streamlining Wind Tunnel. NASA TM-X-72699, August 1975.

32. **Wolf, S. W. D.**: The Design and Operational Development of Self-Streamlining Two-Dimensional Flexible Walled Test Sections. NASA CR-172328, March 1984, 281 pp.

33. **Bailey, A.; and Wood, S. A.**: Further Development of a High-Speed Wind Tunnel of Rectangular Cross-Section. British ARC R&M 1853, September 1938, 16 pp.

34. **Holder, D. W.**: The High-Speed Laboratory of the Aerodynamics Division, N.P.L., Parts I, II and III. Reports and Memoranda No. 2560. December 1946.

35. **Tuttle, M. H.; and Mineck, R. E.**: Adaptive Wall Wind Tunnels - A Selected, Annotated Bibliography. NASA TM-87639, August 1986.

36. **Parker, R. L., Jr.; and Erickson, J. C., Jr.**: Development of a Three-Dimensional Adaptive Wall Test Section with Perforated Walls. Presented at the 50th AGARD Fluid Dynamics Panel Specialists' Meeting on *Wall Interference in Wind Tunnels*, London, England, May 19-20, 1982, AGARD-CP-335 (N83-20957#), paper no. 17, 14 pp.

37. **Morgan, D. G.; and Lee, G.**: Construction of a 2- by 2-Foot Transonic Adaptive-Wall Test Section at the NASA Ames Research Center. *AIAA 4th Joint Fluid Mechanics, Plasma Dynamics and Laser Conference*, AIAA Paper 86-1089, Atlanta, GA, May 12-14, 1986.

38. **Heddergott, A.; Kuczka, D.; and Wedemeyer, E.**: The Adaptive Rubber Tube Test Section of the DFVLR Göttingen. *11th International Congress on Instrumentation in Aerospace Simulation Facilities*, Stanford, California, August 26-28, 1985. In: ICIASF '85 RECORD, IEEE publ. 85CH2210-3.

39. **Ganzer, U.; Igeta, Y.; and Ziemann, J.**: Design and Operation of TU-Berlin Wind Tunnel With Adaptable Walls. *14th Congress of the International Council of the Aeronautical Sciences*, Toulouse, France, September 9-14, 1984. In: Proceedings, vol. 1. (A84-44926), AIAA, 1984, pp. 52-65.

40. **Wolf, S. W. D.; Cook, I. D.; and Goodyer, M. J.**: The Status of Two- and Three-Dimensional Testing in the University of Southampton Transonic Self-Streamlining Wind Tunnel. 50th AGARD Fluid Dynamics Panel Specialists' Meeting on *Wall Interference in Wind Tunnels*, Paper no. 15, London, England, May 19-20, 1982. In: AGARD-CP-335 (N83-20957#).

41. **Blanchard, A.; Payry, M. J.; and Breil, J. F.**: Tests with Three-Dimensional Adaptations in the Rectangular Working Section of the French T2 Wind Tunnel, with a Type AS 07 Swept Wing Half Model Installed. NASA TM-88442, July 1986, 28 pp. Translation of ONERA/CERT R. T. OA 34/3075 (DERAT 12/5015 DN), November 1985, pp. 1-24.

42. **Judd, M.; Wolf, S. W. D.; and Goodyer, M. J.**: Analytical Work in Support of the Design and Operation of Two-Dimensional Self Streamlining Test Sections--Semiannual Progress Report, Oct. 1975-Mar. 1976. NASA CR-145019, July 1976, 67 pp.

43. **Wolf, S. W. D.; and Goodyer, M. J.**: Predictive Wall Adjustment Strategy for Two-Dimensional Flexible Walled Adaptive Wind Tunnel. A Detailed Description of the First One-Step Method. AASU Memo 85/12, January 1986. (NASA CR to be published.)

44. **Lamarche, L.; and Wedemeyer, E.**: Minimization of Wall Interferences for Three-Dimensional Models with Two-Dimensional Wall Adaptation. VKI TN 149 (1984).

45. **Rebstock, R.**: Procedures for Computing Transonic Flows for Control of Adaptive Wind Tunnels. Ph. D. Thesis, NASA TM-88530, January 1987.

46. **Wolf, S. W. D.**: Evaluation of a Flexible Wall Testing Technique to Minimize Wall Interferences in the NASA Langley 0.3-m Transonic Cryogenic Tunnel. *26th AIAA Aerospace Sciences Meeting*, AIAA Paper 88-0140, Reno, Nevada, January 11-14, 1988.

47. **Lewis, M. C.**: Aerofoil Testing in a Self-Streamlining Flexible Walled Wind Tunnel. Ph. D. Thesis, July 1987. NASA CR 4128.

48. **Green, L. L.; and Newman, P. A.**: Transonic Wall Interference Assessment and Corrections for Airfoil Data From the 0.3-Meter TCT Adaptive Wall Test Section. *19th AIAA Fluid Dynamics, Plasma Dynamics and Lasers Conference*, AIAA Paper 87-1431, Honolulu, Hawaii, June 8-10, 1987.

49. **Lesant Y.**: Wall Self Adaptation Process at Mach 1.2 - Final Report. ONERA-RTS-31/3075-AY-402, April 1985. In French, N86-28968#.

50. **Chevallier, J. P., Mignosi, A.; Archambaud, J. P.; and Seraudie, A.**: T2 Wind Tunnel Adaptive Walls--Design, Construction, and Some Typical Results. La Recherche Aerospatiale (English Edition), no. 4, July/August 1983, pp. 1-19.

51. **Stephens, T.**: Design, Construction and Evaluation of a Magnetic Suspension and Balance System for Wind Tunnels. NASA CR-66903, November 1969.

52. **Cortner, A. H.; and Brown, M. D.**: Design and Initial Calibration of a Magnetic Suspension and Balance System for Wind Tunnel Models at the Arnold Engineering Development Center. In: Proceedings of ARL Symposium on *Magnetic Wind Tunnel Model Suspension and Balance Systems*. ARL 66-0135, July 1966.

53. **Britcher, C. P.**: Some Aspects of Wind Tunnel Magnetic Suspension Systems with Special Application at Large Physical Scales. NASA CR-172154, September 1983.

54. **Dahlen, G. A.; and Brundin, C. L.**: Wall Temperature Effects on Rarefied Hypersonic Cone Drag. *13th International Symposium on Rarefied Gas Dynamics*, Novosibirsk, USSR, July 1982.

55. **Bloom, H. et al**: Design Concepts and Cost Studies for Magnetic Suspension and Balance Systems. NASA CR-165917, July 1982.

56. **Boom, R. W.; Eyssa, Y. M.; McIntosh, G. E.; and Abdelsalam, M. K.**: Magnetic Suspension and Balance System Study. NASA CR-3802, July 1984.

57. **Boom, R. W. et al**: Magnetic Suspension and Balance System Advanced Study. NASA CR-3937, October 1985.

58. **Martindale, W. R.; Butler, R. W.; and Starr, R. F.**: Study on Need for a Magnetic Suspension System Operating with a Transonic Wind Tunnel. NASA CR-3900, May 1985.

59. **Britcher, C. P.; Goodyer, M. J.; Eskins, J.; Parker, D.; and Halford, R. J.**: Digital Control of Wind Tunnel Magnetic Suspension and Balance Systems. *12th International Congress on Instrumentation in Aerospace Simulation Facilities*, Williamsburg, Virginia, June 1987.

60. **Britcher, C. P.; Goodyer, M. J.; Scurlock, R. G.; and Wu, Y. Y.**: A Flying Superconducting Magnet and Cryostat for Magnetic Suspension of Wind-Tunnel Models. *Cryogenics*, April 1984.

61. **Roberts, P.; and Tcheng, P.**: Strain-Gage Balance Calibration of a Magnetic Suspension and Balance System. *12th International Congress on Instrumentation in Aerospace Simulation Facilities*, Williamsburg, Virginia, June 1987.